CHALMERS
UNIVERSITY OF TECHNOLOGY

SYNTHETIC GAS BENCH AND SIMULATION TOOL CHARACTERISATION OF THREE-WAY CATALYTIC CONVERTER

Master's thesis in Innovative and Sustainable Chemical Engineering

EMMA WESTERBORN

DEPARTMENT OF CHEMISTRY AND CHEMICAL ENGINEERING
CHALMERS UNIVERSITY OF TECHNOLOGY
Gothenburg, Sweden 2022
www.chalmers.se

Master's thesis 2022

Synthetic Gas Bench and Simulation Tool Characterisation of Three-Way Catalytic Converter

EMMA WESTERBORN

CHALMERS
UNIVERSITY OF TECHNOLOGY

Department of Chemistry and Chemical Engineering
The Competence Centre for Catalysis
Chalmers University of Technology
Gothenburg, Sweden 2022

Synthetic Gas Bench and Simulation Tool Characterisation of Three-Way Catalytic Converter
EMMA WESTERBORN

Supervisor: Mats Laurell (Aurobay) and Prof. Magnus Skoglundh (Chalmers)
Examiner: Prof. Magnus Skoglundh

Master's Thesis 2022
Department of Chemistry and Chemical Engineering
The Competence Centre for Catalysis
Chalmers University of Technology
SE-412 96 Gothenburg
Telephone +46 31 772 1000

Cover: Commercial monolith heterogeneous catalyst brick seen from above.

Typeset in LaTeX
Gothenburg, Sweden 2022

Synthetic Gas Bench and Simulation Tool Characterisation of Three-Way Catalytic Converter

EMMA WESTERBORN
Department of Chemistry and Chemical Engineering
Chalmers University of Technology

Abstract

A three-way catalytic converter (TWC) is a necessary tool in order to lower the emissions from stoichiometric combustion such the emissions from petrol-fueled vehicles. The TWC can efficiently reduce the three main pollutants: CO, hydrocarbons (HC) and nitrogen oxides (NOx). Once the TWC is used it may suffer from deactivation, which affects the performance of the catalyst.
This master thesis was done in collaboration with Aurobay and the experiments were performed at the Competence Centre for Catalysis at Chalmers University of Technology. Three catalyst samples, one from a stabilised fresh commercial three-way catalyst and two from different parts of a rapidly aged TWC were investigated using flow-reactor experiments in a synthetic gas bench (SGB) to study the effect of the deactivation procedure. These results showed a clear axial distinction in the degree of deactivation in the catalyst. Following this was a simulation using the commercial simulation program Gamma Technology Suite (GT-suite), where the kinetic parameters of the model were calibrated and optimised against the experimental results of the stabilised fresh catalyst. For the optimisation, constant temperature steady state tests at three different temperatures were used, as well as oxygen storage tests to calibrate the reactions on the cerium oxide sites of the catalyst. The optimised model parameters were then validated against a SGB light-off test. The optimised simulation model was also tested against a SGB light-off test for the deactivated catalyst sample to investigate what measures had to be taken to correctly simulate the ageing procedure. Finally, the same model parameters were tested against values from a motor bench test performed at Aurobay, to study how the model would hold up against a more real life-like test.
The parameters for the cerium oxide sites could not be optimised but instead left to their baseline parameters. In the end, the final optimised model showed good simulation results for the reduction of NOx but not as good results for the oxidation of CO and HC. When tested against the experimental values of the deactivated catalyst sample, the parameters from the optimised model performed better than the baseline parameters, despite the model being optimised on the stabilised catalyst. The same was seen for the motor bench experiments, however the simulated values still showed a substantial difference from the actual results. The optimisation processes show that the precious metal dispersion factor has a considerable effect on the final simulated results, and it might be worth to focus more on calibrating these parameters rather than optimising the kinetic parameters as was the main focus in this report. The thesis therefore concludes that further investigations are desired to quantify how crucial the need of unique experimental parameter setting actually is.

Acknowledgements

Firstly I would like to express my deepest gratitude to my supervisor Mats Laurell at Aurobay and Prof. Magnus Skoglundh at Chalmers for all of their support, feedback and discussions during this thesis.
I would also like to thank Aurobay for giving me the opportunity to perform the master thesis and the support from everyone there that I had the pleasure to meet. Same goes to Competence Centre for Catalysis at Chalmers University of Technology. Special thanks goes to Duc-Khanh Nguyen, without whom this work would not have been possible, as well as to Ghodsieh Isapour Toutizad and Joonsoo Han for all their help with the experimental part of this thesis.
Lastly I would like to thank my partner for all of his support during these busy months, and to my dear friends for the invaluable moral support and always being available when it was needed the most.

Emma Westerborn, Gothenburg, June 2022

List of Acronyms

Below is the list of acronyms that have been used throughout this thesis listed in alphabetical order:

AFR	Air-to-Fuel Ratio
FTIR	Fourier Transform Infrared Spectroscopy
GT	Gamma Technology
OSC	Oxygen Storage Capacity
PGM	Platinum Group Metals
SGB	Synthetic Gas Bench
TWC	Three-Way Catalytic Converter

Contents

List of Figures

List of Tables

1

Introduction

As countries try and battle the impacts of modern society on the climate as well as the human health, legislations are tightening. This is especially the case regarding emissions from vehicles, where EU is releasing more and more stringent regulations.

If the combustion in the engine would work perfectly at all times, then the exhaust gas from the car would mainly consist of water, carbon dioxide (CO_2) and heat. However, due to incomplete combustion of the fuel, as well as impurities or additives, there are multiple other compounds leaving the engine [4]. These compounds include; Carbon monoxide (CO), unburned hydrocarbons (HC), nitrogen oxides (NOx), hydrogen (H_2) and oxygen (O_2) [4][5][6]. Of these, CO, HC and NOx are seen as the primary pollutants [4], since CO is highly toxic while HC and NOx can react together in the presence of sunlight to create smog, which highly reduces the air quality [5][6]. To combat these, vehicles are equipped with a catalytic converter. The so called Three-way catalytic converter (TWC) is a vital component to lower the before mentioned emissions from petrol engine cars, named due its ability to efficiently reduce all three of the primary pollutants at the same time.

Multiple factors control the efficiency of the TWC and while most of them are tuned in the construction of the catalyst or by controlling the engine exhaust, the deactivation (or ageing) of the catalyst happens during the usage and is inevitable.The ageing happen when the catalyst is being exposed for high temperatures or impurities in the fuel [5][7] and will accumulate throughout the use of the car with high impact on the TWCs performance. As the catalytic converter has to last the average lifetime of a car (160 000 km), engine manufacturers need to prove that the performance is high enough to meet the legislation, even at the end of its lifetime. Measurements and characterisation of the emissions are therefore done on a deactivated catalyst, ideally on a catalyst that has been aged in a vehicle to obtain as correctly measurements as possible. However, vehicle deactivation of a catalyst takes time and resources, and most manufacturers will instead utilise ”rapid ageing methods” as a faster and less expensive alternative. In some cases vehicle ageing is not possible if new applications are to be tested. The rapid ageing method often vary between different manufacturers, and will sometimes include iterations where the catalyst is tested to see if it matches the deactivated pattern of a vehicle aged catalyst, and if not the deactivation process will continue. Despite this, rapid ageing methods poses a problem of not accurately predicting the right deactivation pattern

and the emission values may therefore be misinforming. For these reasons, it is of interest for the manufacturers to find a way to more correctly deactivate the TWC, to ensure that the same trend on emissions will be seen for the customers as in the lab setting. However, as there are many parameters that can affect the kinetics of reactions in a catalyst, testing a range of different settings manually would be extremely time consuming. Here the use of a commercial simulation tool can be of huge asset, and can be used to investigate how alternating parameters will effect final emissions to plan out the deactivation procedure. Despite the existence of pre-determined kinetic parameters for the model, it is recommended to tune the simulation to experimental data for the specific catalyst in focus. For this reason an experimental campaign ought to be performed. Commercial simulation programs are used in many different fields, and for the transport sector it can be used to model from the whole car or just a single catalyst brick. By understanding in detail how rapid ageing affects the catalyst and being able to mimic that with a commercial simulation program, a possibility could be that the ageing method can be modelled ahead before executed. Thereby saving time and resources that today go into a more iterative form of ageing, while achieving a more exact deactivation.

1.1 Scope

In this project, Two Three-Way catalysts provided by Aurobay are examined: one fresh stabilised commercial catalyst, and one that has been aged by a rapid ageing method. Both catalyst have the same specifications and are only differing in the level of deactivation. One sample from the fresh catalyst and two samples from the aged catalyst, one from the front side and one from the rear side, are investigated using flow-reactor experiments in a Synthetic Gas Bench (SGB) and the results from these tests are compared. Following this, a simulation model is optimised based on performed experiments of the stabilised catalyst. The final optimised model is then validated against temperature ramp test as well as tested on the results of the deactivated catalyst samples, to investigate the measures that have to be taken for modelling deactivation. Finally, the model is also validated against earlier motor bench tests performed at Aurobay on a stabilised catalyst. The Master Thesis project is performed in collaboration with Aurobay.

The thesis focuses on comparing the conversion between the different catalyst samples as well as between the experimental and simulated data, however does not focus on evaluating the performance of the catalyst.

The aim of the thesis is to gather experience of calibration of the simulation tool and baseline parameters built into the GT suite package. This is achieved by investigation of the deactivation with regards to the SGB experiment results, as well as by trying to obtain a working simulation model that can accurately predict conversion efficiency of the TWC.

2

Background

In this chapter the necessary background will be explained.

2.1 Three-Way Catalytic Converter

Catalysts are used in a wide range of different fields and the introduction of the right catalyst into a system can make it possible for reactions to take place at a lower temperature range and help favour otherwise non-selective reactions [1]. For some processes, a catalyst is essential for the reaction to happen at all. The reaction mechanism for a catalysed reaction can briefly be described by Figure 2.1 below.

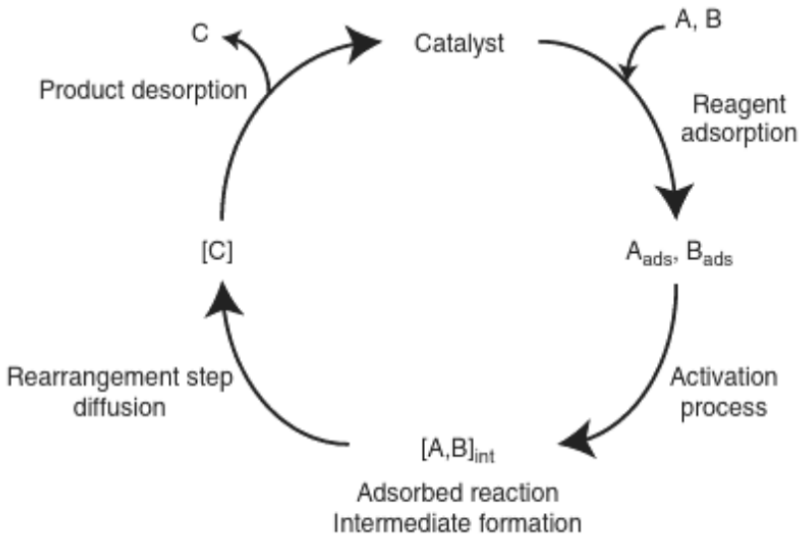

Figure 2.1: The steps of a catalytic reaction [1]

Exhaust After Treatment System (EATS) is a collective word for the part of a vehicle setup that is responsible for the treatment of the engine exhaust in order to reduce the harmful emissions of a vehicle. Part of the EATS is a catalytic converter, an essential tool in order to lower the emissions from a car engine. For a petrol engine vehicle a Three-Way Catalytic Converter (TWC) is utilised. The TWC is a heterogeneous monolith catalyst named due to its ability to efficiently reduce three

main pollutants from the petrol engine: Hydrocarbons (HC), Carbon Monoxide (CO) and Nitrogen oxides (NOx). These pollutants are seen as the most important to target for reduction due to their local health hazard [8]. The primary reactions that happen in the TWC are shown below [6][8]:

$$2CO + O_2 \rightarrow 2CO_2 \tag{2.1}$$

$$HC + O_2 \rightarrow CO_2 + H_2O \tag{2.2}$$

$$2NO + 2CO \rightarrow 2CO_2 + N_2 \tag{2.3}$$

Reactions 2.1 and 2.2 are oxidation reactions while reaction 2.3 is a reduction reaction.

With the right conditions, the TWC can have conversion efficiencies of up to 95% assuming normal usage of the car [5][9]. In order to work well the catalyst need to be at sufficiently high temperature [10], which is an issue during the start up of the engine when the catalyst is cold. It is estimated that a majority of the emissions, up to 80% [10][5], from the car happens during the start up period. As the catalytic converter once being fully heated while have high performance, the area of interest to study is the light-off period due, when the catalytic converter is functioning at its worst. Therefore, in order determine the performance of a catalyst, a "light-off test" is commonly done, where the tail-pipe emissions are measured starting from a cold catalyst until the catalyst is fully heated. From this the light-off temperature can be determined, that being the temperature at which the conversion is 50% [11]. The light-off temperature is usually around 250°C [9] but differs from catalyst to catalyst. A catalyst with low light-off temperature is desirable as it directly translates to high conversion of the pollutants during this critical phase.

2.1.1 Rate of Reaction

For any chemical reaction, the reaction rate can be expressed with the Arrhenius reaction rate expression seen below. When a catalyst is present, it changes the rate of the reaction and therefore the reaction parameters [1]. However, it does not affect the the equilibrium between the reactants and products.

$$r = A * e^{-\frac{E_A}{RT}} \tag{2.4}$$

Where R is the gas constant (8,314 J/(mol K)), T is temperature (K), A is the **pre-exponential factor** and E_A is the **activation energy**. A higher temperature will result in a higher value of the reaction rate and therefore a higher conversion.

At a constant inlet temperature the reaction rate will be constant. For this reason there is an infinite number of pre-exponential factors and activation energies that will result in the same rate constant at the specific temperature. Determining the kinetic parameters of a reaction based only on one constant temperature is therefore not feasible if those parameters are to be used for any other temperature. Solving for the kinetic parameters can be done by a linear regression for experimental results

of the reaction rate a at least two temperatures. By taking the natural logarithm of Eq. 2.4, the pre-exponential factor and the activation energy can be found by plotting the natural logarithmic value of different reaction rates versus the inverse of the temperature. See Eq. 2.5 and Figure 2.2 below.

$$ln(r) = ln(A) - \frac{E_A}{R} * \frac{1}{T} \tag{2.5}$$

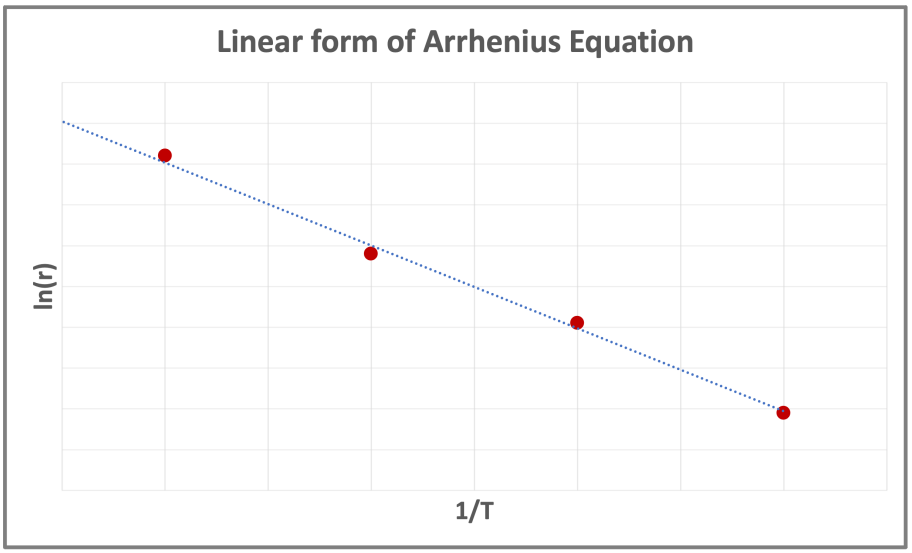

Figure 2.2: Example of linear regression with the use of Arrhenius equation to find the pre-exponential factor and the activation energy

2.1.2 Precious metal active sites

In a TWC, the catalytic reactions take place on Platinum Group Metal (PGM) active sites, usually Palladium (Pd), Platinum (Pt) and/or Rhodium (Rh). In the early development of catalytic converters for cars, the most common was to use a Pt/Pd mix because of the metals ability to catalyst the oxidation of HC and CO, before Rh was included due to the discovery of its role in the reduction reaction of NOx. The catalyst in focus for this study is a Pd/Rh mix, which shows advantages in HC conversion and lower light-off temperature compared to Pt/Rh [5]. The loading of the PGM as well as the ratio between the different metals will differ for different applications of the catalyst.

2.1.3 Air-to-Fuel ratio

As mentioned before, the reactions in the TWC are a mix of reduction and oxidation reactions. The oxidation reactions benefit from a higher concentration of oxygen while it at the same time hinders the reduction reaction, and vice versa. Air is used as the oxygen source for the combustion of the fuel in the engine, and altering the air intake into the engine will have a direct effect on the efficiency of the TWC.

A theoretical "Air-to-fuel" ratio (AFR) can be calculated to determine the exact amount of air that is needed for combustion of the type of fuel used. For petrol this value is generally 14,7:1.

$$\lambda = \frac{AFR_{real}}{AFR_{theoretical}}$$

By comparing this to the actual AFR, one can see if there is an excess of air or of fuel in the engine. The quotient between theoretical and actual is called lambda (λ), where a $\lambda > 1$ shows a lean condition (excess of oxygen) and a $\lambda < 1$ shows a rich condition (excess of fuel). In lean conditions the conversion of NOx is therefore low while the conversion of CO and HC stays high as oxidation reactions are favoured, and in rich conditions the opposite trend is noticed. It is wanted to keep the value of λ close to 1, the stochiometric point, as this is where the TWC will work most efficiently for conversion of all three pollutants, since the environment will favour both reduction and oxidation reactions. [5][12].

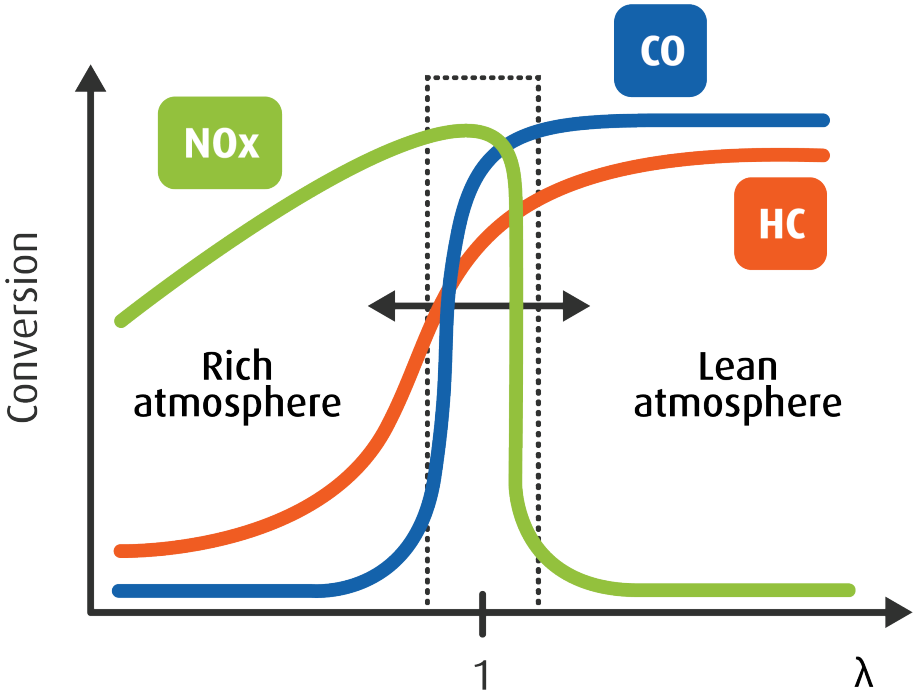

Figure 2.3: Schematic image of the effects on the conversion of NOx, CO and HC depending on the value of λ [2].

The values close around $\lambda = 1$ where the efficiency is still high is referred to as the "lambda window", see the area in the dotted lines in Figure 2.3. λ-sensor by the catalyst connected to the software of the engine will control the air-intake to stay inside of the λ-window. However, the margins are small and as driving can be very unpredictable, only controlling the air intake is not adequate enough.

This is where the cerium-sites (Ce) on the catalyst brick in the TWC comes in [5]. Cerium oxide works as an oxygen storage compound and can release and bind

oxygen as needed, by the formation of Ce_2O_3 and CeO_2 respectively. The cerium interaction with the gas species of focus can be seen in Equation 2.6-2.11 below. This acts like an oxygen buffer and makes it possible for the TWC to reach high efficiency. The TWCs ability to store oxygen can be described by the TWCs "Oxygen Storage Capabilites" (OSC).

$$2Ce_2O_3 + O_2 \rightarrow 4CeO_2 \tag{2.6}$$

$$Ce_2O_3 + NO \rightarrow 2CeO_2 + 0,5N_2 \tag{2.7}$$

$$CO + 2CeO_2 \rightarrow Ce_2O_3 + CO_2 \tag{2.8}$$

$$H_2 + 2CeO_2 \rightarrow Ce_2O_3 + H_2O \tag{2.9}$$

$$C_3H_6 + 12CeO_2 \rightarrow 6Ce_2O_3 + 3CO + 3H_2O \tag{2.10}$$

$$C_3H_8 + 14CeO_2 \rightarrow 7Ce_2O_3 + 3CO + 4H_2O \tag{2.11}$$

2.2 Catalyst deactivation

Catalyst deactivation, also called ageing, has great effect on the TWCs performance. Deactivation is characterised by a decrease in activity and/or selectivity, and can be caused by loss, blockage or hindered accessibility to the active sites [13]. The catalyst ageing can be a result of thermal ageing, chemical poisoning, mechanical damage and catalyst coking [7], where thermal ageing and chemical poisoning are seen as the most affecting for TWCs [5].

2.2.1 Thermal ageing

Thermal ageing refers to the catalyst deactivation due to high temperatures for an extended period of time [5][7]. For TWCs this includes the process of **sintering**, which can be seen as the most influencing deactivation factor for the catalytic converter [5]. Sintering happens when smaller clusters of PGM grows into bigger particles on the expense of smaller. This happens either when particles migrates and then coalesces with each other, or by atoms moving from one particle to another (Ostwald ripening) [13]. Sintering is irreversible and will lead to a loss of active surface on the catalyst, as multiple smaller particles will have a higher total surface area than one bigger (despite having the same total mass). Thermal deactivation will also affect the oxygen storage capabilities, due to the low thermal stability of CeO_2 [5] as well as can lead to phase change of the coating, Al_2O_3, another loss of active catalyst surface [7].

2.2.2 Chemical poisoning

The cause of chemical deactivation of the catalyst is found in impurities in the fuel or caused by chemical additives (such as lubricating oils) [5][7] or even from impurities in the air intake [13]. Chemical poisoning is the result of adsorption of the impurities on the catalyst, leading to the active sites no longer being available

for the adsorption of reactants, see Figure 2.1. Poisoning of the catalyst could be reversible depending on the cause of the poisoning. An impurity that adsorbs to the surface at low temperatures could potentially desorb when the catalyst is exposed to high temperatures [13]. For example, poisoning of sulphur is reversible while phosphor and calcium poisoning leads to irreversible effects.

2.3 Ageing Methods

Due to the high effect that the deactivation has on the performance of the catalyst, it is required for the manufacturers to prove the function of the catalyst even at the end of its lifetime. Tail-pipe emission tests are performed on deactivated catalysts, to study the catalyst "at its worse". To obtain deactivated catalyst for studying, a need of ways to deactivate catalysts in an accurate way is required. Three different methods for rapid ageing of a catalyst are: Vehicle ageing, Burner ageing or TWC bench ageing [7][14].

2.3.1 Vehicle Ageing

Vehicle ageing is done by installing the catalyst in a vehicle that is then run according to a set cycle for approximately 160 000 km. Usually, the vehicle is placed on a chassis dynamometer on which the resistance can be changed to simulate the load at different speeds, as well as placing a fan in front for the simulated wind resistance. In this way one can tailor the driving cycle to mimic a normal life time of driving [7][14]. The benefit of this ageing method is that the catalyst is deactivated in the most real-life way as possible. However, the disadvantages is the long time period needed (around 6-9 months) and with that a large cost due to staff, fuel, vehicle damage and tyre wearing [7].

2.3.2 Burner Ageing

The burner ageing is the only one of the three mentioned methods that does not utilise an actual engine. Instead, the catalyst is installed in a burner that provides an exhaust flow with components and heat similar to the engine exhaust [7][14]. By altering temperature, injecting air and oil and controlling other settings, the environment is altered to simulate a real driving case. With the burner the air-to-fuel ratio and temperature can be controlled in a precise way, leading to a time efficient ageing method where it usually only takes a few days, up to a week to finish [7] depending on cycle chosen. The deactivation results on the catalyst will however differ somewhat to a vehicle aged catalyst. Another shortcoming is that the exhaust gas components in the burner compared to actual engine exhaust are slightly different [7][14]. However, as the deactivation is mainly due to impurities and temperature, it is not clear what effect the exhaust components have on deactivation [7].

2.3.3 Engine Bench Ageing

Another common rapid ageing of a catalyst is the so called ”Bench ageing method”, also the deactivation method used for the commercial deactivated catalyst studied in this thesis. Bench ageing takes place in an engine bench and by altering air-to-fuel ratio, engine speed, simulating engine misfires and adding high levels of poisoning, the goal is to mimic the deactivation in a shorter time period [7]. The catalyst bed is typically kept above 950°C to mimic the thermal deactivation. Advantages of this method is its efficiency and the short time period that it takes [14][7]. Bench ageing can take between a few days to up to a month depending on method used, and one can age several catalytic converters at the same time. This together with that the engine bench can also be easily reused, leads to a substantial lower total cost compared with vehicle ageing. However, the main disadvantage is that the deactivation of the catalyst show a different deactivation pattern from vehicle aged catalyst [7].

2.4 Simulation and Optimisation of Chemical Reactions

When dealing with a complex system of multiple chemical reactions taking place all at once, computer simulation is a highly useful tool. If used correctly, it has huge advantages with giving the potential of testing out a wide range of different design options in order to choose the most promising settings for further studies. There are many different commercial simulation programs that can be used for a range different application. In this thesis the application ”Gamma Technolgy Suite” (GT-suite) will be used.

In order to acquire an accurate and reliable simulation model for catalytic reactions, the model has to be optimised and validated against an experimental campaign. Flow reactor experiments performed in a Synthetic Gas Bench (SGB) can be utilised to conduct experiments as it gives full control of the gas species entering the reactor. This makes it possible to isolate the reactions taking place on the catalyst and calibrating them individually.

2.4.1 Genetic Algorithm

Genetic algorithm, or GA for short, is a stochastic algorithm that can be utilised for optimisation problems, such as optimisation of a model to fit experimental data as is the case in this thesis. GA was developed with Charles Darwin’s theory of evolution in mind [15], the theory that living creatures have evolved over several generations based on a criterion that made them the fittest for survival. The most successful children would manage to grow up, meet a mate, reproduce and their offspring would carry the successful gene mixed with other capabilities from the other parent. This mix from two parents would either increase or decrease the likelihood of survival for the children, and thus the evolution continues.

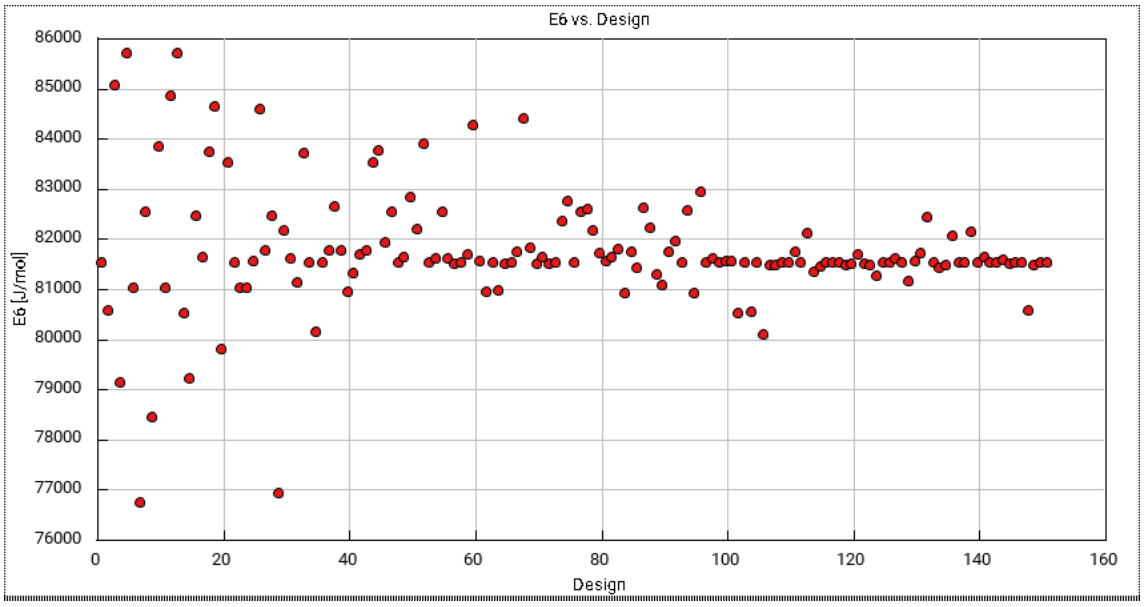

Figure 2.4: An example on the convergence by the GA algorithm

GA works in a similar way. It all starts with a population, consisting of individuals where every individual is a possible solution. The algorithm examines each member of the population, each solution, and decides on their fitness level, which is determined by how good of a solution it is. Members deemed to have low fitness level are discarded, and members with good levels are then paired up to ”reproduce” and create ”children”, new solutions. The hope is that the new solutions will contain the optimal parts from the parent solution, and that at least some of them will then become an even better solution. Once the GA has run through the first population, it starts over with all the new created solutions, a new generation of solutions. Mutation are added in the reproducing of new solutions in order to add randomness to the solutions and to hinder the creation of too many identical ”children” [15].

The GA can run for a set number of generations or until a solution is found that is ”good enough”. While running the optimisation process, the idea is that each generation will be more fit than the last, leading to a convergence of the values for the model parameters that are set. An example of this can be seen in Figure 2.4. The GA can be used for finding values that have to fit multiple cases, for example different temperatures.

2.4.1.1 Objective function

In order for the algorithm to find a solution, it needs a definition of the solution, what value the algorithm is striving to find. By defining an objective function based on the square difference of the experimental outlet values and the simulated outlet values, the aim of the algorithm will be to minimise this function. The best solution is therefore the one closest to zero. This is demonstrated in Eq. 2.12 below.

$$F_{obj} = \int_{t_{start}}^{t_{end}} \sum [(X_{exp,out} - X_{sim,out})^2 + (Y_{exp,out} - Y_{sim,out})^2 + (Z_{exp,out} - Z_{sim,out})^2] dt \tag{2.12}$$

Where X, Y and Z represent different gas species, depending on which species are targeted.

2.4.2 Optimisation of Reaction Rate Parameters

As explained in Section 2.1.1, calibration of the reaction rate parameters have to be performed for multiple temperatures in order to achieve a correct result. A manual way of performing this calibration will be to utilise the linear regression based on reaction rate and temperature, as explain in the same section. However, an advantage of using the GA is its possibility to optimise based on multiple separate results, and this can be utilised to optimise the kinetic parameters. By using a "Case Sweep"-method, where each case represent the experimental values at different temperatures, the GA will strive to find one solution that fits all cases.

When case sweep is used for optimisation, an objective function is created for each case setup (for example for each temperature case). A mean value of these objective functions will then represent the final solution which is subject for minimisation.

$$F_{obj,\ case\ sweep} = \frac{F_{obj,\ case\ A} + F_{obj,\ case\ B} + [...]}{\text{Number of cases}} \tag{2.13}$$

This method can be used to optimise the kinetic parameters instead of manual calibration.

2.4.3 Simulation of Ageing

In GT-suite, the main way of expressing the deactivation level of the catalyst is by decreasing the available active sites in the model, both for the cerium sites as well as PGM sites. This is done by altering the value of the "Active Site Density", which is exactly what the name suggests, the density of the active sites. The active site density is expressed in number of moles per total volume of the reactor, mol/m^3. The active site density depends on the dispersion factor, which is the ratio of active site to total sites.

$$\text{Active Site Density} = \frac{\text{Loading of site element * Dispersion factor}}{\text{Atomic weight}} \tag{2.14}$$

The active site density can either be added directly into the model or let the model calculate it themselves if the loading of site element and atomic weight is known. The porosity is not taken in account.

3

Synthetic Gas Bench - Methodology and Result

In the following chapter the Synthetic Gas Bench (SGB) test scheme as well as the results will be presented. Following in Chapter 4 will be description of the GT-suite simulations.

The synthetic gas bench experiments were performed at the Competence Centre for Catalysis at Chalmers University of Technology. The inlet gas flow was controlled by mass flow controllers, one per gas species, and the concentration of the outlet gas was measured with an FTIR (Fourier Transform Infrared Spectroscopy analyser). Eight gas species are chosen for use in the SGB; Propane (C_3H_8), Propylene (C_3H_6), Hydrogen (H_2), Oxygen (O_2), Nitrogen Oxide (NO), Carbon monoxide (CO), Carbon dioxide (CO_2) and evaporated water (H_2O). Argon (Ar) was used as the inert gas in all the experiments. A limitation of FTIR is that it cannot detect O_2 or H_2, and thus there will be no experimental values for these species.

3.1 Earlier Engine Bench Experiments

In order to perform experiments on the catalyst samples in the SGB that would be similar to the environment in an engine, typical compositions in engine exhaust gas had to be found. This was achieved by analysing earlier motor bench experiments performed at Aurobay. At Aurobay, the general way of testing the catalyst is to perform an engine bench test. These were performed on a stabilised commercial catalyst and for a lean phase mixture (λ=1,02) as well as a rich phase mixture (λ=0,98). As the full fuel mixture contain more gas species than will be used in the SGB experiments, only the values of the relevant species were extracted.

From the engine bench test a value of the total unburnt hydrocarbons (uHC) were provided. In order to acquire the concentrations of propylene and propane separately, the values had to be transferred to a C3 basis with the use of a so called "C3 fraction", Y_{C3}.

To find Y_{C3}, Eq. 3.1 was used where Y_{C3} was altered until the calculated mean value of lambda (λ_{calc} matched with the experimental value.

$$\lambda_{calc} = \frac{2X_{CO2} + X_{CO} + 2X_{O2} + X_{H2O}}{2(X_{CO2} + X_{CO} + 3Y_{C3}X_{uHC}) + 0,5(2X_{H2} + 2X_{H2O}) + [6Y_{C3H6} + 8(1 - Y_{C3H6})] * Y_{C3}X_{uHC}} \quad (3.1)$$

Where Y_{C3H6} is the ratio between propylene and propane. Assuming a ratio of 0.8 it was found that Y_{C3}=0,3 matched the lambda measurements. Once these fractions were decided, the dry measurements were recalculated into wet measurements using the water concentration, as well as recalculating the air mass flow to mass flow of fuel. The final concentrations extracted from the engine bench test and used in the SGB are seen in Table 3.1.

Table 3.1: The gas species concentration (%) extracted from the engine bench experiments.

Mixture #	**C_3H_6**	**C_3H_8**	**H_2**	**NO**	**CO**	**O_2**	**CO_2**	**H_2O**
Lean phase mixture	0,035	0,01	0,06	0,3	0,25	0,7	15	10
Rich phase mixture	0,04	0,011	0,225	0,18	0,8	0,2	15	10

3.2 Experimental phase

The following section will explain the experimental phase. First the sample preparations will be described, followed with descriptions of the different test schemes. The final part of this section will explain the data analysis of the results.

3.2.1 Sample preparations

From the two catalyst bricks supplied by Aurobay, samples with a dimensions of **15mm width x 15 mm length** was cut out. At the front side from both catalyst bricks (seen from mass flow direction) a 15 mm slice was cut out, as well as from the rear side of the aged catalyst. Two samples were then cut from the middle position of the slices (one primary sample for experiment and the other kept as a backup). The samples were named: S1 & S2 (stabilised fresh catalyst), Cf1 & Cf2 (aged catalyst front side) and Cb1 & Cb2 (aged catalyst back side).

Figure 3.1: The two catalyst bricks supplied from Aurobay, stabilised to the left and the bench aged brick to the right.

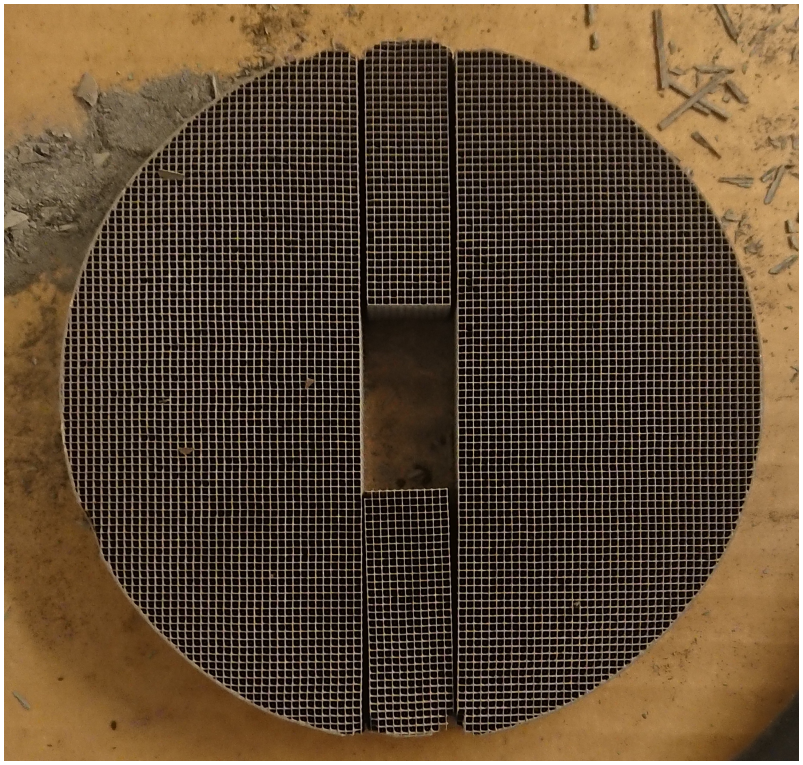

Figure 3.2: The placement of the samples taken from the catalyst brick.

The sample of the catalyst is placed in a quartz tube wrapped in insulation as seen

in Figure 3.3 below. The quartz tube is surrounded by a spiral coil through which the heating is supplied with electric heating. The gas flow was preheated to 191°C before it entered the quartz tube, and then heated to the desired temperature inside the tube. The heating was measured by two thermocouples: The first thermocouple measured the heat of the gas before the catalyst sample, and was placed 1,5 cm past the catalyst sample. The second was put in the middle of the catalyst sample to measure the temperature inside the catalyst. The placement is visible in Figure 3.4.

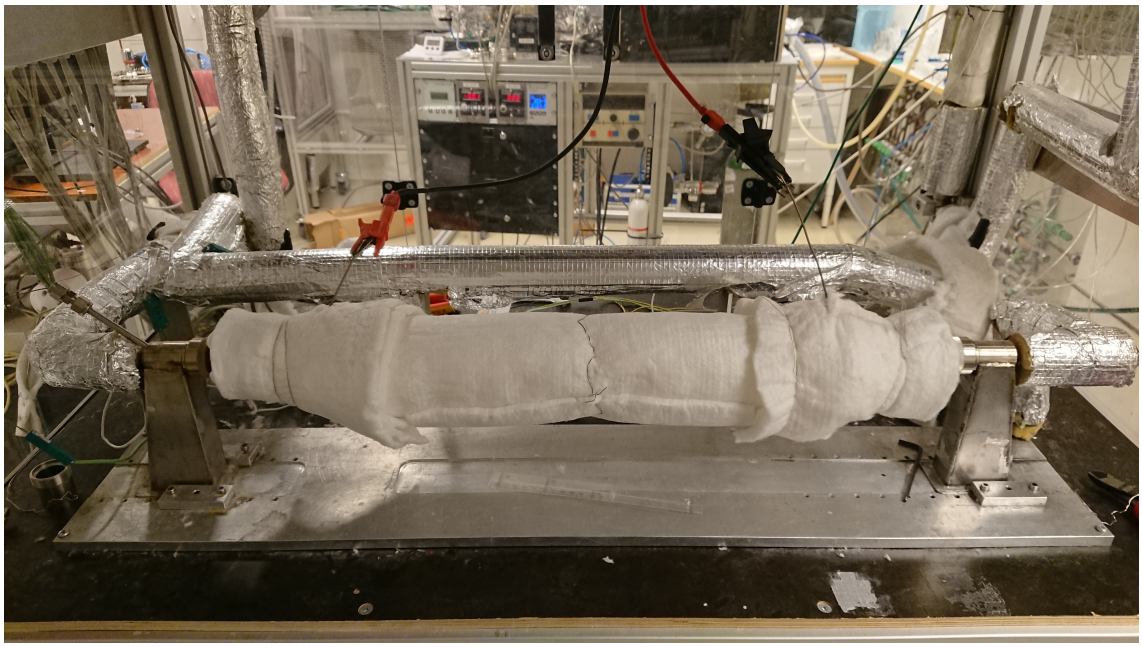

Figure 3.3: The synthetic gas bench rig used in this thesis

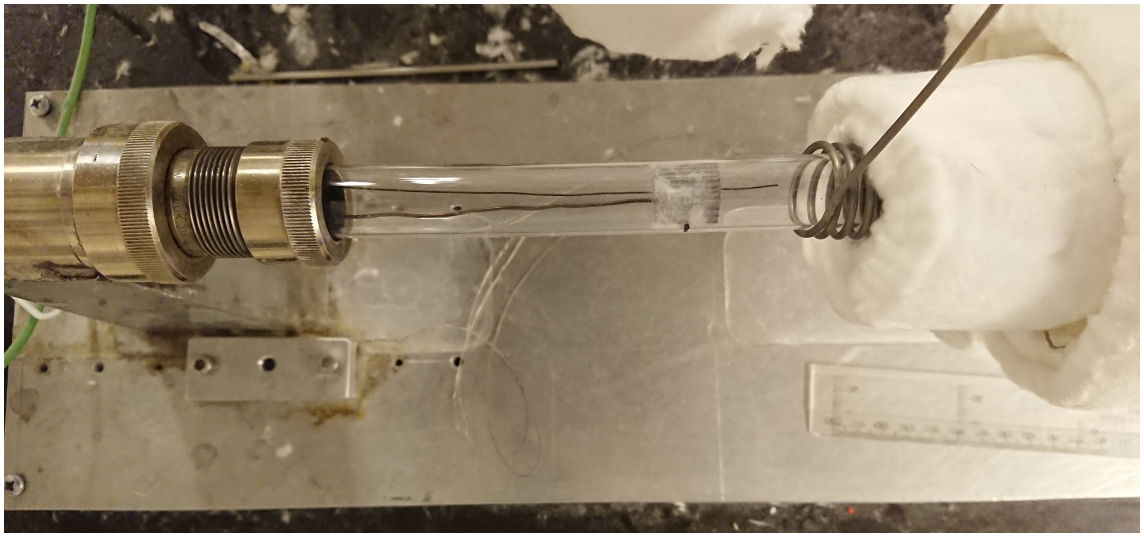

Figure 3.4: The placement of the sample in the quartz tube. The gas flow is coming from the right.

3.2.2 Planning of Experiments

The following test schemes were performed in the SGB,

- Oxygen storage test
- Constant Temperature Steady State test
- Temperature ramp test

The oxygen storage and constant temperature steady state test will be used for calibration and optimisation of the simulation model, while the temperature ramp test are to be used for validation of the finished model.

Below follows a more detailed description of each of the experimental tests.

3.2.2.1 Oxygen Storage Capacity Test

Oxygen storage capacity (OSC) test were performed to determine the oxygen storage performance of the catalyst. These test aimed to be used to target the reactions at the Cerium site, reactions 10-15 in table 4.1. As there are multiple gas species that can act to store or reduce the storage of oxygen on the cerium sites, two different experimental tests were performed, see below.

OSC experiment 1:

- Lean phase consisting of 1% O_2
- Rich phase consisting of 0.9% CO

OSC experiment 2:

- Lean phase consisting of 1% O_2 and 0.1% NO
- Rich phase consisting of 0.9% CO, 0.3% H_2 and 0,05% C_3H_6

The duration of the lean phase was 60 seconds, before switching to the rich phase for 60 seconds and then repeating once more for each phase. The test were performed at 4 different constant inlet temperatures: 200°C, 300°C, 400°C and 500°C, with a total volume flow of 1500 ml/min.

3.2.2.2 Steady state test

To optimise the model parameters for the reactions active on the PGM sites of the catalyst, a series of test were performed at constant inlet temperature, letting the system reach steady state. By performing these test, it is possible to better isolate the reactions used in the simulation model and optimise them one by one, compare to when a full fuel mixture is used. In total 7 different gas mixtures were tested, see Table 3.2, at 5 different temperature levels: 200°C, 300°C, 400°C, 500°C and

600°C. The volume flow at the inlet was 1200 ml/min. Not shown in the table is the Ar-flow that accounted as the inert filler gas.

Table 3.2: The gas species concentration (%) of the 7 different gas mixtures used for the constant temperature steady state test.

Mixture #	**C_3H_6**	**C_3H_8**	**H_2**	**NO**	**CO**	**O_2**	**CO_2**	**H_2O**
1	0,04	0,01	-	-	-	0,2	15	10
2	-	-	0,08	-	0,3	0,15	15	10
3	-	-	-	-	2	-	15	10
4	0,09	0,03	-	-	-	-	15	10
5	-	-	0,35	0,05	1	-	15	10
6	0,1	0,04	-	0,2	-	-	15	10
7	0,1	0,04	0,25	-	-	1,275	15	10

The steady state experimental tests were conducted for all 7 gas mixtures at the highest temperature level before letting the SGB cool down to repeat at next temperature. The scheme for testing one gas mixture was as follows:

- Pre-treatment of catalyst with 1,5% O_2 for 300 seconds
- 100% Ar flow for 300 seconds (to minimise contamination with the oxygen flow)
- Gas mixture #1 for 300 seconds
- 100% argon flow for 300 seconds (to minimise contamination)

The steps were repeated with all the gas mixtures in same order as can be seen in Table 3.2. The pre-treatment of the catalyst was to ensure a fully oxidised catalyst so that the prerequisites were the same at every temperature level.

3.2.2.3 Temperature ramp test

Temperature ramp tests were performed to evaluate the crucial light-off period. The temperature ramp tests were performed on three mixtures, mixtures 8, 9 and 10 seen in Table 3.3, with a total volume flow of 1500 ml/min. Mixture #8 and #10 were provided from the motor bench test as explained in Section 3.1. Mixture #9 was created to find a stochiometric mixture.

Lambda value was calculated using Equation 3.1.

The system was first heated up to 500°C and then pre-treated with oxygen for 300 seconds. The catalyst sample was exposed for the full gas mixture at constant temperature for 600 seconds before left to cool down to 100°C. It was then left at

Table 3.3: The gas species concentration (%) of the three different gas mixtures used for temperature ramp experiments.

Mixture #	C_3H_6	C_3H_8	H_2	NO	CO	O_2	CO_2	H_2O
8	0,035	0,01	0,06	0,3	0,25	0,7	15	10
9	0,05	0,02	0,15	0,1	0,5	0,6	15	10
10	0,04	0,011	0,225	0,18	0,8	0,2	15	10

Table 3.4: The λ-value of the mixtures assigned for temperature ramp test.

Mixture #	Calculated λ-value
8 - Lean phase mixture	1,02
9 - Stochiometric mixture	1
10 - Rich phase mixture	0,98

100°C for 20 minutes and thereafter the rig was heated back up to 500°C, with a speed of 5°C/min. The procedure was repeated for all three gas mixtures.

The simulation model will be evaluated using the temperature ramp test after having been optimised from the oxygen storage capacity and steady state tests. To limit the scope of the report, only the light-off period (100°C-500°C) will be in focus, and the cool down period will not be studied in detail.

3.2.3 Experimental Data Analysis

After gathering the experimental data the next step was to evaluate and calibrate the outlet concentration data from the FTIR. In order to be able to perform an FTIR calibration, a calibration test scheme was done in an empty tube beforehand. A fraction between the inlet concentration value and the actual outlet FTIR measured value was calculated and this fraction was then used to calibrate all the following experimental data. Ideally calibration measurements should be done at a range of different concentration values for every gas species, but due to time restraint it was limited to a few selected values for each gas species.

The actual inlet values were obtained as mass flow from the MFC and were recalculated into mole fraction in order to be compared with the outlet concentration measurements.

3.3 Results

Below a selection of the experimental results will be presented.

3.3.1 Constant Temperature Steady State Experiment

Below are the experimental results of CO conversion for Mixture #3, catalyst sample S1, to show the conversion in % at each tested temperature level.

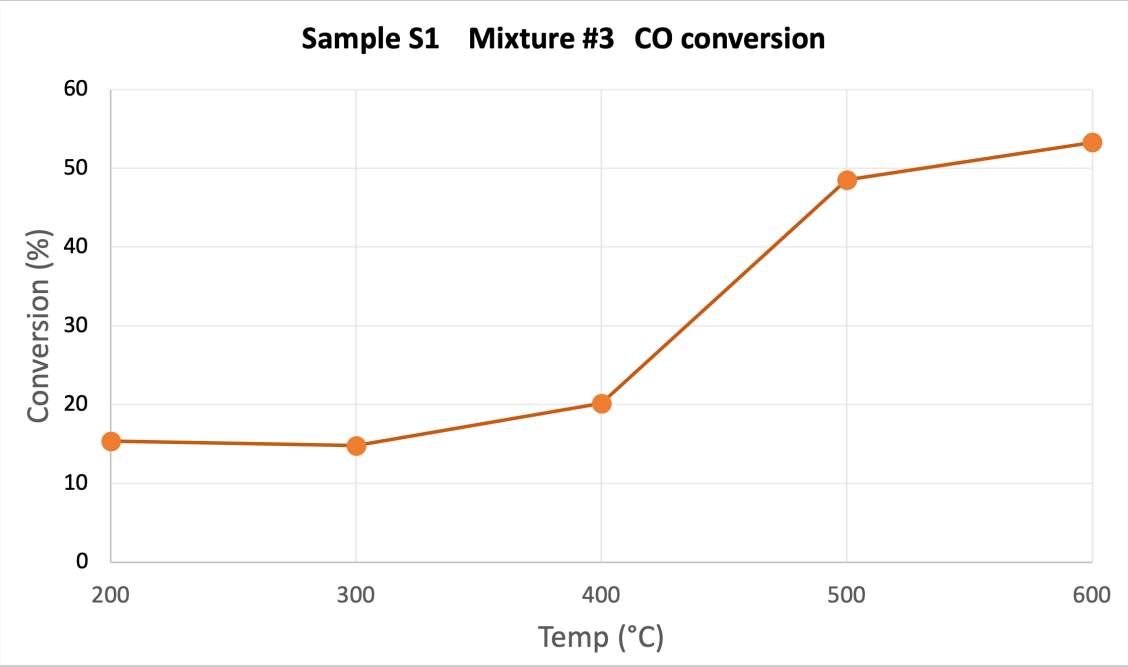

Figure 3.5: The conversion of CO

The non-linear rise in conversion with a higher temperature seen in Figure 3.5 can be understood as the Arrhenius equation is exponential (see Eq. 2.4) and small changes in temperature can have a big impact on the conversion. The experimental results from the constant temperature test will be utilised further in Chapter 4, for optimisation of model parameters.

3.3.2 OSC experiments

From the OSC experiments the oxygen storage of the catalyst was quantified using the experimental outlet concentration of CO_2. In Figure 3.6 an example of the results from the OSC experiments is shown, here for sample S1 at 500°C.

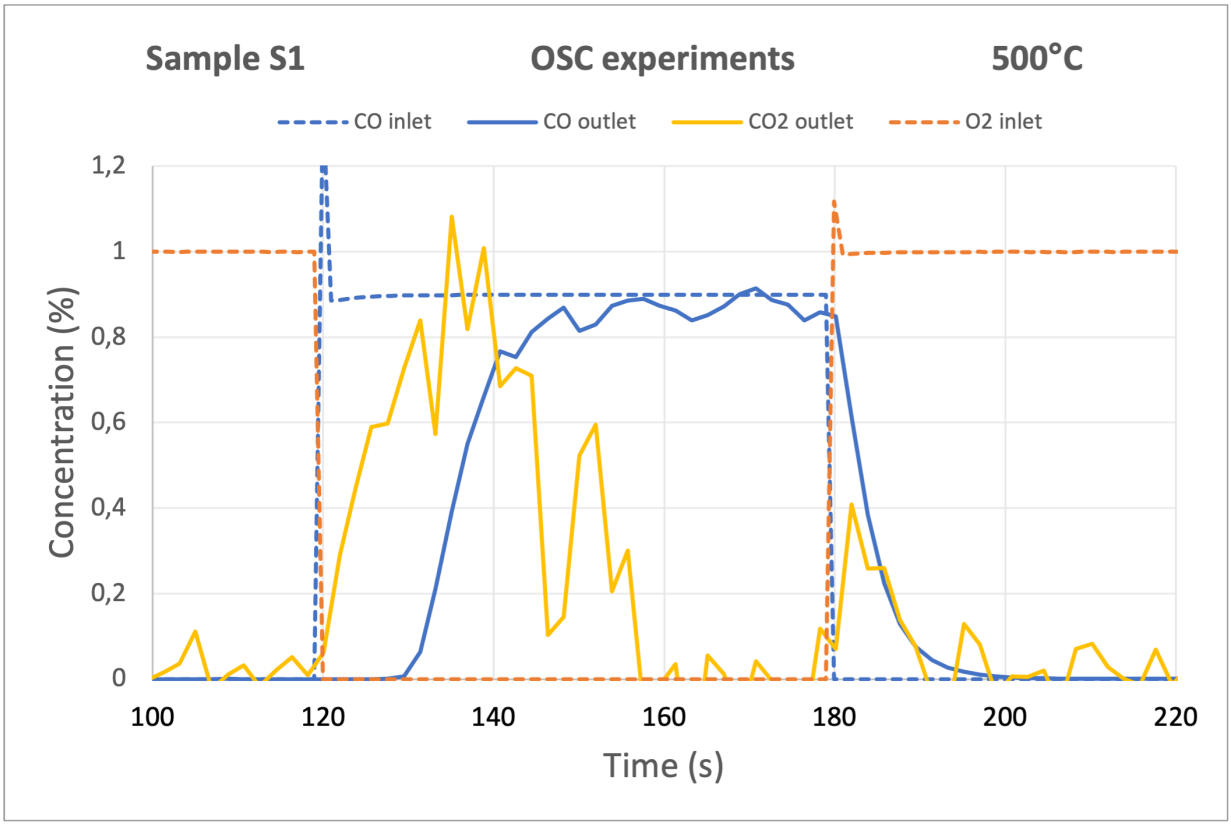

Figure 3.6: Results from OSC experiment 1, using Sample S1 at 500°C

As can be seen in Figure 3.6, when CO is introduced at 120 seconds, the CO_2 level starts steadily increasing as the CO is reacting with CeO_2. As the amount of CeO_2 is decreasing, so is the amount of created CO_2 until there is only CO in the outlet again. One can also see a second peak of the CO_2 concentration at 180 seconds, this is due to the introduction of O_2 with CO still in the reactor, as is seen in the graph.

Looking at Eq. 2.6 (see Section 2.1.3), ratio of O_2 to CeO_2 is 1:4. Following, 1 mole of CO and 2 mole of CeO_2 is needed to produce 1 mole of CO_2 (Eq. 2.8). This means that the ratio of stored O_2 to CO_2 is 1:2. By taking the integral of the CO_2 outlet curve, the amount of stored oxygen could thereby be determined. The result of this for all the samples at the different temperatures can be seen in Figure 3.7.

As expected, the amount of oxygen stored is the highest for the fresh catalyst, sample S1, and the lowest for the front of the aged catalyst, sample Cf1. The values for the back side of the aged catalyst, Cb1, is somewhere in between, showing that it has not been as affected by the deactivation as the front side.

Looking into the effect of temperature on the oxygen storage, the samples S1 and Cb1, are showing a peak at 400°C. For Cf1, the level of oxygen storage is increasing as the temperature increases. Similar results are shown in an earlier work performed by Jian Gong et al. ([16]), with a peak of oxygen storage at 400°C for the fresh sample, but not the deactivated sample.

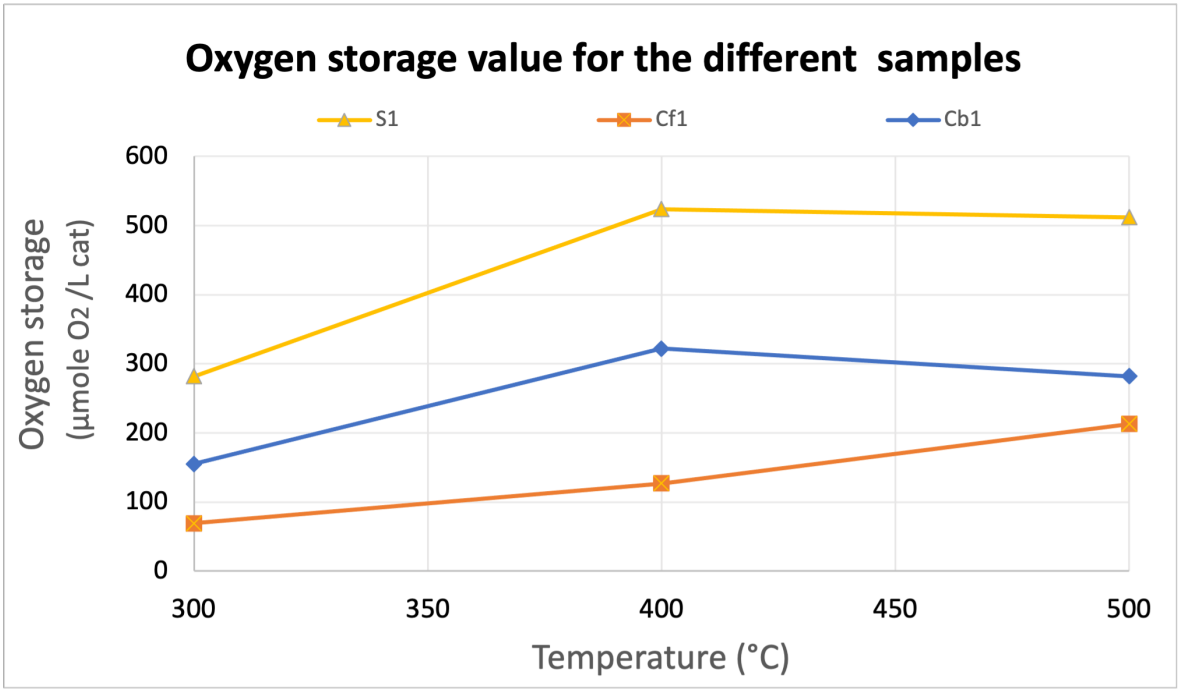

Figure 3.7: Oxygen storage value (µmole O_2/L cat) for the different samples at different temperatures.

3.3.3 Temperature Ramp Experiment

In this section the results of the temperature ramp experiments will be presented, and the focus will be on comparing the light-off test for the three different mixtures and all three catalyst samples. These results are later used for validation of the simulation model, further explained in Chapter 4. As can be seen in Table 3.4, Mixture #8 is a lean phase mixture, Mixture #9 is a stochiometric mixture and Mixture #10 is a rich phase mixture.

As the most crucial time, when the emissions are the highest, is during the warm-up phase, it is important to have a catalyst as effective as possible at the lowest possible temperature. For this reason, the comparison of the catalyst samples will be based on temperature needed for the conversion to go up and not the conversion when the catalyst is fully heated (500°C).

3.3.3.1 CO conversion

Comparing the CO conversion over temperature, see Figure 3.8, the conversion is higher for the lean phase than for the rich phase mixture (comparing M#8 and M#10) for all the samples. This is in line with what was discussed in Section 2.1.3, where a lambda value above 1 (lean phase) is beneficial for conversion of CO. Looking at the stabilised sample, S1, the effect of the temperature on conversion is not very different between the lean phase mixture and the stochiometric mixture, which suggest that M#9 is indeed around the stochiometric value. However the difference is greater between the lean phase and stochiometric mixture for the deactivated

samples, especially the shape of the curve for the front side sample, Cf1. After 200°C, the conversion is not changing as swiftly when the temperature is rising, and it is even kept steady at 60% for about 25°C. This could be due to a production of CO (which is possible in a TWC, see Table 4.1 presented in the next chapter). However as this is mainly seen for Cf1, which is believed to be the most deactivated sample and therefore with the least amount of active sites, this could also be due to a lack of available sites and the oxidation of CO not being favoured at that temperature.

Comparing the samples to each other, it is clear that the stabilised fresh sample (S1) is performing the best in terms of higher conversion at lower temperatures. The back side of the aged catalyst (Cb1) is however not differing too much from the stabilised sample, and for the case of M#9 the light-off temperature is even slightly lower for Cb1 compared to S1, due to the shape of the curve. As mentioned, Cf1 is believed to be the most deactivated sample which is confirmed in Figure 3.8, as it is performing the worst compared to the other samples. When performing bench ageing, a high amount of poison is added in a short amount of time. It is likely that the impurities will poison or foul the beginning of the catalyst as that is simply what it reaches first, and less impurities will exist in the exhaust gas once it reaches the end of the catalyst. However, it is judged that when using bench ageing method, the rear side will be more affected by thermal deactivation than the front side. Worth to mention is that for the overall performance of the catalytic converter the importance is the performance of the whole brick, and axial differences are assumed to happen in vehicle deactivation as well. In order to study the difference between rapid ageing methods, further investigation including different catalyst bricks with different methods of deactivation would be needed. In the end however all samples reach 100% conversion when temperatures are high enough (except for M#10).

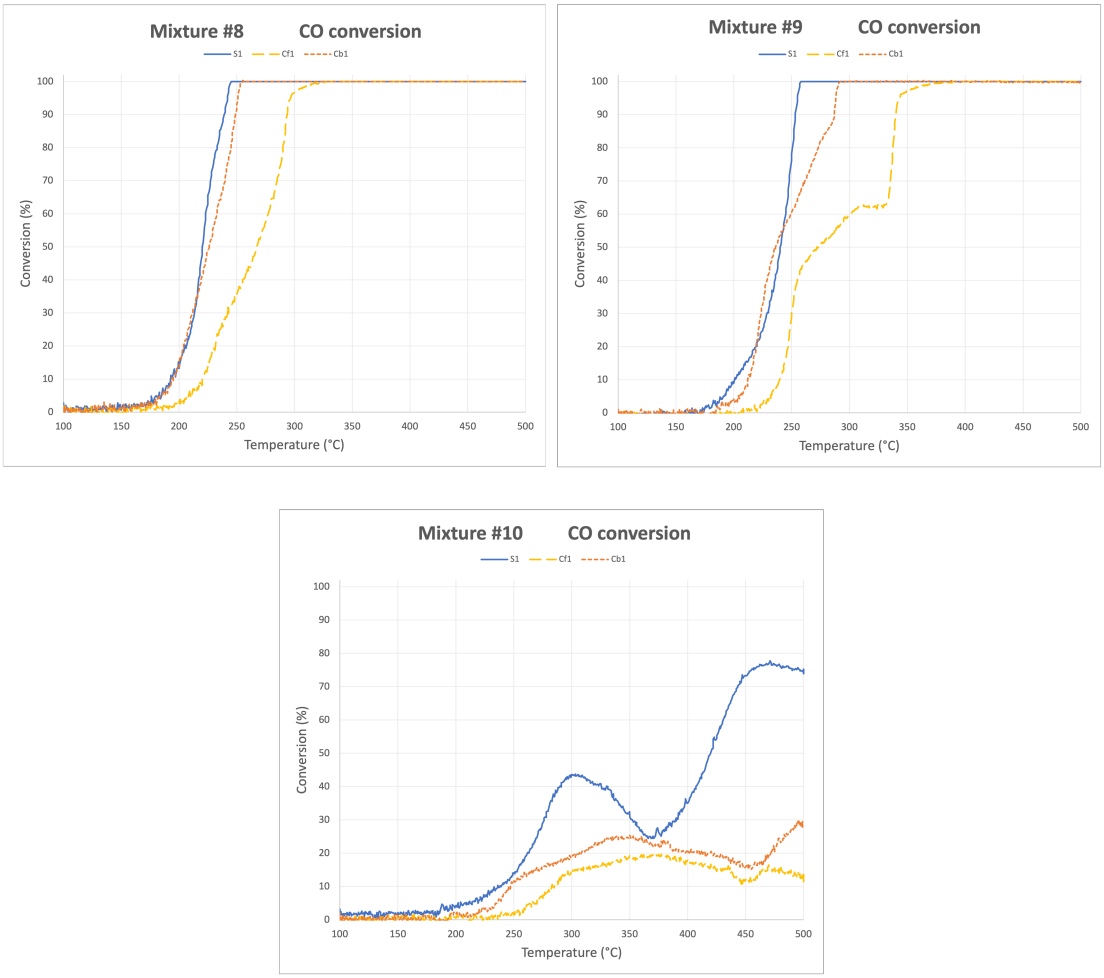

Figure 3.8: Conversion of CO over temperature for all three catalyst samples and the three mixtures #8, #9 and #10.

3.3.3.2 C_3H_6 and C_3H_8 conversion

For the conversion of propylene, C_3H_6, the samples are all performing better for the lean phase mixture compare to rich phase, as expected due to reasons discussed for the CO conversion. However the C_3H_6 conversion is not as affected as the CO conversion was in the rich phase mixture and still reach high levels. For the stochiometric mixture there is a slight increase in light off temperature compared to the lean phase mixture, an increase that is higher for the deactivated samples compared to the stabilised sample. When comparing the samples, the front side of the catalyst is once again proven to be the most deactivated sample.

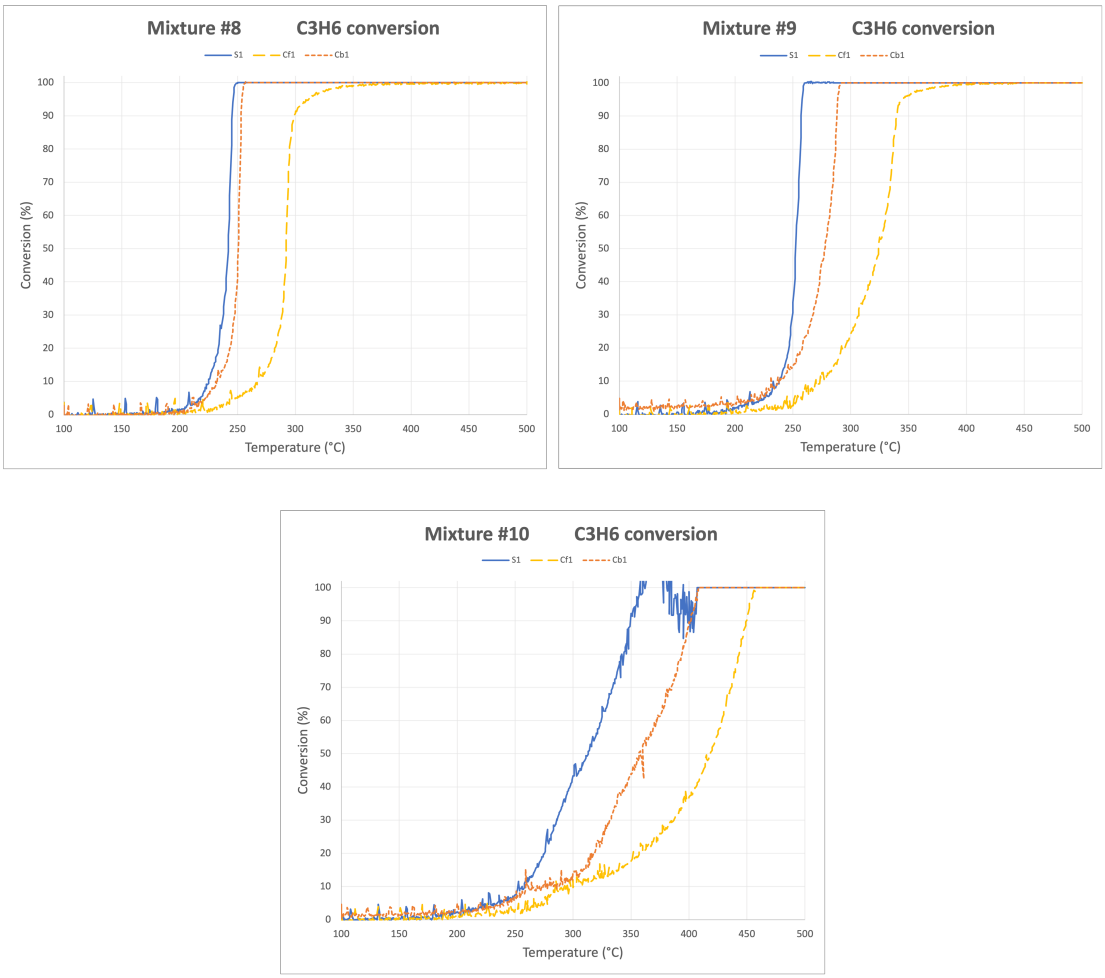

Figure 3.9: Conversion of C_3H_6 over temperature for all three catalyst samples and the three mixtures #8, #9 and #10.

Looking instead at the conversion of propane, C_3H_8, the conversion in generally worse than for propylene, due to the double bond in propylene making it more reactive than propane. Similar trends as what was seen for the conversion of C_3H_6 is seen for C_3H_8 as well, as expected.

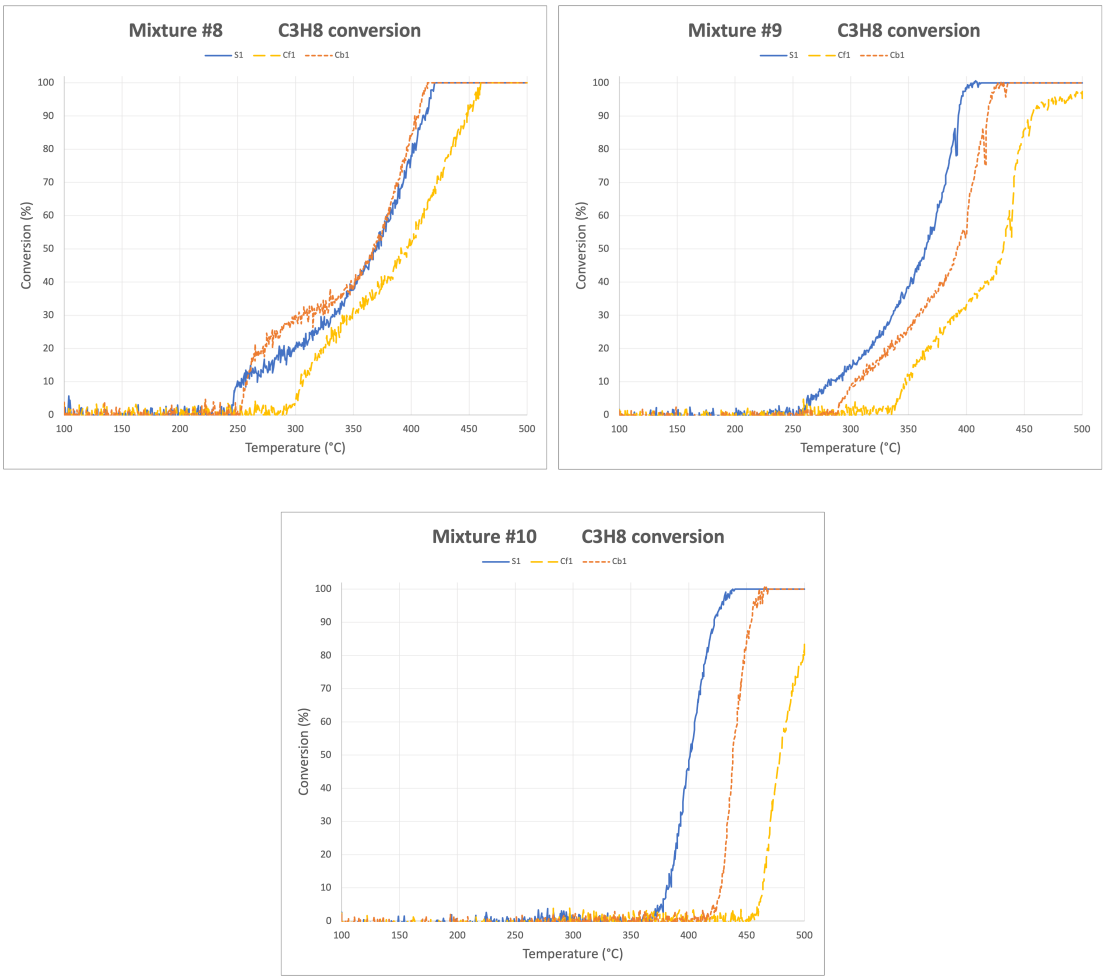

Figure 3.10: Conversion of C_3H_8 over temperature for all three catalyst samples and the three mixtures #8, #9 and #10.

3.3.3.3 NO conversion

For the NO conversion the conversion is very low for the lean phase mixture and high for the rich phase mixture, due to the rich phase environment being beneficial for the reduction of NO.

Comparing the shape of the curves at the different mixtures, the conversion of NO is changing more drastically than what could be seen for the other gas species. For example if looking at M#9, the conversion is drops down in two occasions. For M#10 similar trend can be seen, however not as extreme. The conversion of NO seems to be more sensitive to the temperature change than what has been seen for the other gas species.

Comparing the samples, they all have a similar shape but at different temperatures, with the performance being worse for the deactivated samples as seen before.

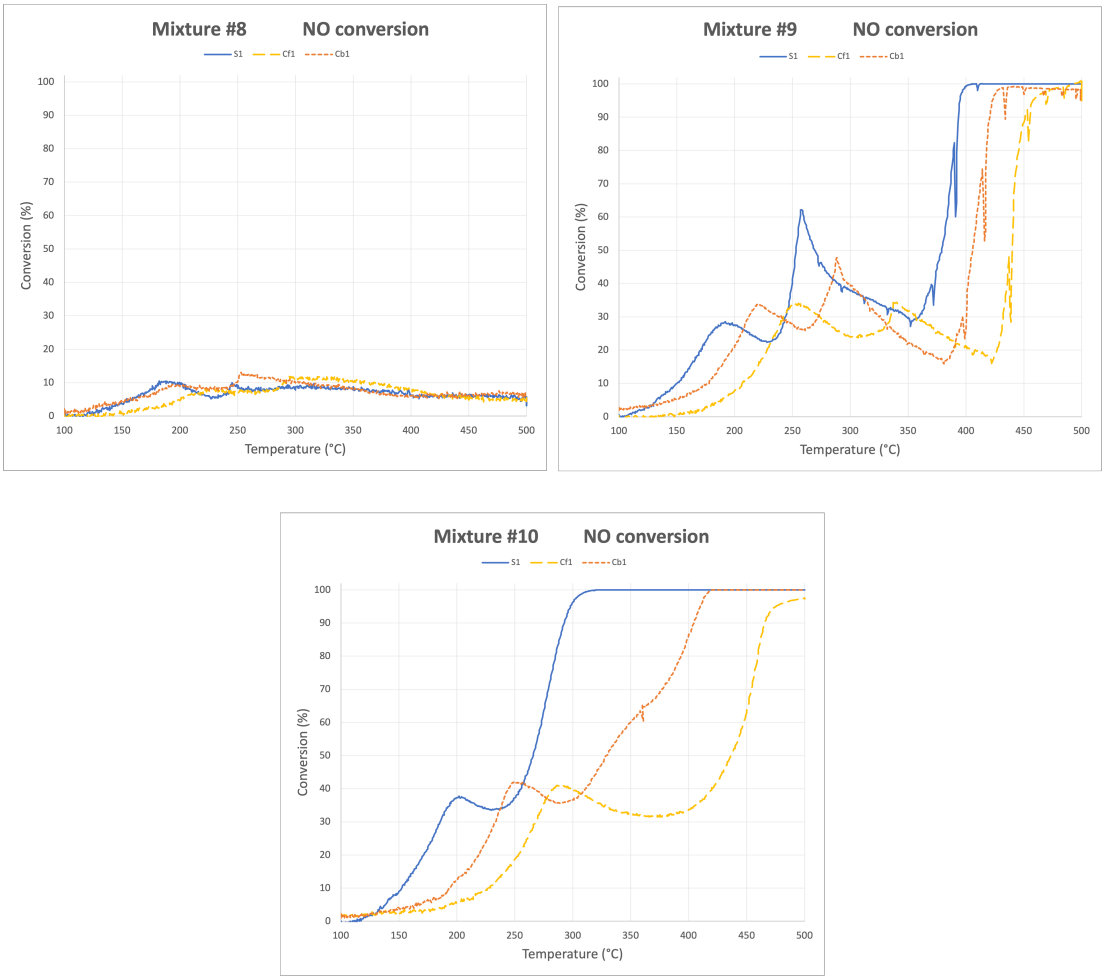

Figure 3.11: Conversion of NO over temperature for all three catalyst samples and the three mixtures #8, #9 and #10.

The next step was to perform an optimisation of the model parameters in the commercial software GT-suite, which will be explained in the following chapter.

4

GT-suite Simulation

Following the experiment phase was the attempt of creating a good simulation model in the commercial software Gamma-Technology suite (GT-suite). For the reaction rate parameters (pre-exponential factor and activation energy), the baseline values are taken from a study by Ramanatha and Sharma [3]. The reactions used in the simulation setup and the baseline model parameters can be seen in Table 4.1 and Table 4.2.

Table 4.1: The reactions targeted in GT-suite and their associated site elements.

Reaction #	**Associated Site Element**	**Reactants**	**Products**
1	PGM	$CO+0.5O_2$	CO_2
2	PGM	$C_3H_6+4.5O_2$	$3CO_2+3H_2O$
3	PGM	$C_3H_8+5O_2$	$3CO_2+4H_2O$
4	PGM	$H_2+0.5O_2$	H_2O
5	PGM	$CO+NO$	$CO_2+0.5N_2$
6	PGM	C_3H_6+9NO	$3CO_2+3H_2O+4.5N_2$
7	PGM	H_2+NO	$H_2O+0.5N_2$
8	PGM	$CO+H_2O$	CO_2+H_2
9	PGM	$C_3H_6+3H_2O$	$3CO+6H_2$
10	Cerium	$2Ce_2O_3+O_2$	$4CeO_2$
11	Cerium	Ce_2O_3+NO	$2CeO_2+0.5N_2$
12	Cerium	$CO+2CeO_2$	$Ce_2O_3+CO_2$
13	Cerium	$C_3H_6+12CeO_2$	$6Ce_2O_3+3CO+3H_2O$
14	Cerium	$C_3H_8+14CeO_2$	$7Ce_2O_3+3CO+4H_2O$
15	Cerium	H_2+2CeO_2	$Ce_2O_3+H_2O$

Table 4.2: The baseline kinetic parameters [3].

Reaction #	**Pre-exponential factor [A]**	**Activation energy [EA] (J/mol)**
1	5,54*10^{13}	121450
2	1,92*10^{15}	129530
3	6,40*10^{15}	165160
4	1,81*10^{15}	111450
5	2,86*10^{9}	52374
6	2,99*10^{11}	80063
7	7,88*10^{10}	69237
8	1,80*10^{5}	43926,258
9	1,23*10^{5}	81920
10	2,94	5296
11	792	25101
12	18,2	30680,453
13	13,6	39070
14	17,7	39680
15	2,85	31768

4.1 TWC Simulation Model

The model used in this thesis is adapted from a previously made model. Due to this scope of this thesis focusing on the catalytic converter, a standalone model for the TWC was used. A simplified version of the final model can be seen in Figure 4.1.In the ”inlet”, #1, the inlet composition, gas temperature and volume flow are defined. ”Cone-1”, #2a acts to connect the inlet flow with the inlet of the catalyst pipe while ”Cone-2”, #2b, connect the outlet of the catalyst pipe with the outlet environment. In #2a the distance of the outer thermocouple to the catalyst brick is added. In the catalyst brick, #3, the catalyst sample is defined. Finally in ”TWC”, #4, the information regarding the chemical reactions such as the baseline parameters is added.

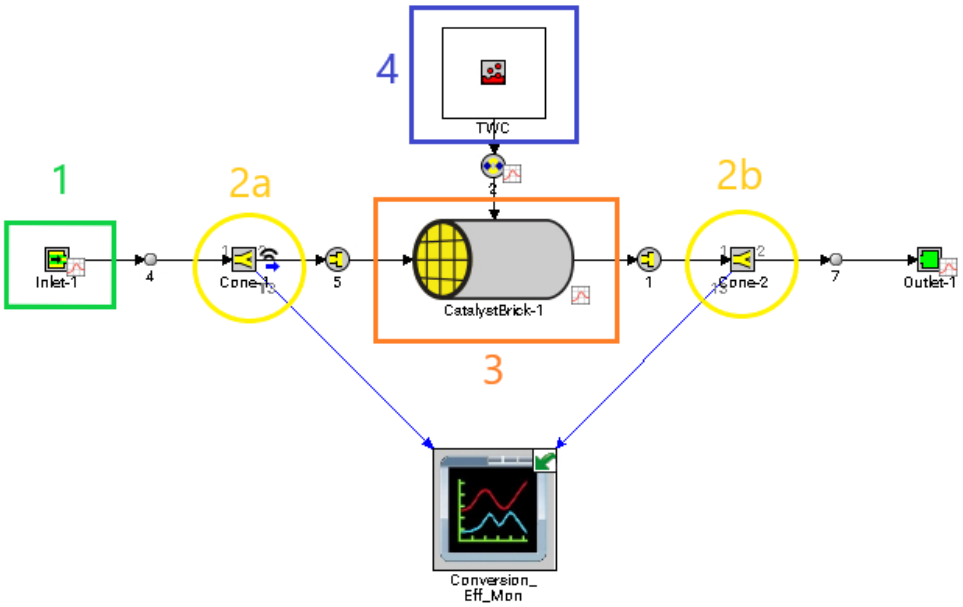

Figure 4.1: A simplified version of the final model.

The final model can be seen in Figure 4.2. The main added part, marked with a blue square, is used for the optimisation process. As can be seen in the model, it was decided to optimise based on the measurements of total hydrocarbons (THC) and not propane and propylene separately. A monitor for monitoring the simulated catalyst temperature against the experimental catalyst temperature was added onto the model, as well as a λ calculator by the inlet.

The known catalyst data, see Table 4.3, was added in the in the model and the discretisation length was assumed to be 1/40 of catalyst length. The master time step was sat as **1,8 seconds** to match frequency of the outlet measurements from the FTIR. The loading of the PGMs as well as the ratio between Pd/Rh was included in the model.

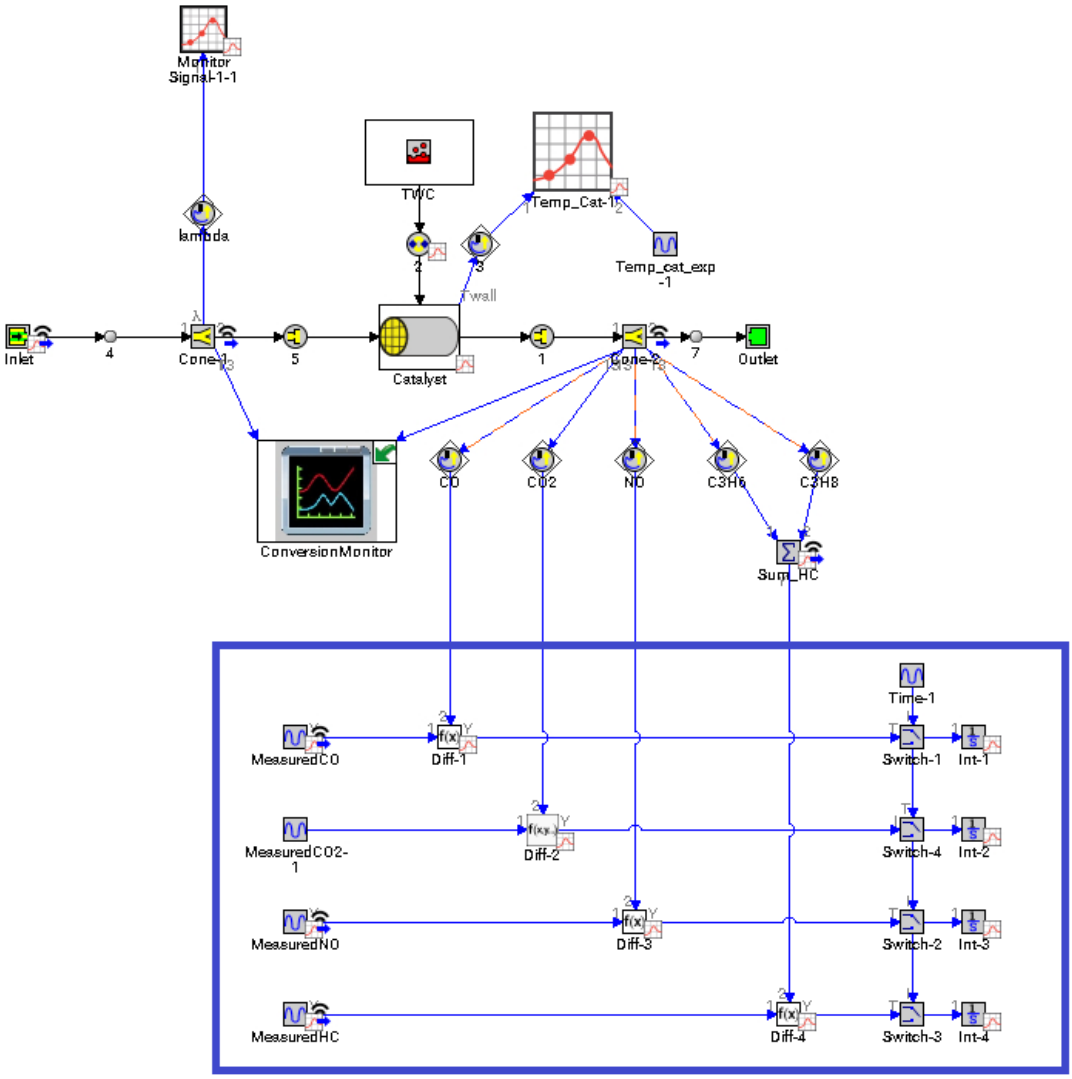

Figure 4.2: The final simulation model setup.

Table 4.3: Catalyst data added in the GT-suite model

Catalyst sample length	15 mm
Frontal diameter	15 mm
Cell density	400 cpi
Substrate Wall Thickness	0,11 mm
Substrate material	Cordierite

4.2 Optimisation process

The following parameters will be subject for optimisation:

- PGM dispersion factor and Cerium active site density
- Pre-exponential factor and Activation energy

Theoretically, the inhibition function, which takes into account the competition amongst the species whose reactions are catalysed on the same PGM site, could also be subject of optimisation but will not be altered in the scope of this thesis.

As the loading and atomic weight of the PGM site is known, the dispersion factor can be altered to acquire the Active site density for the PGM site. For the cerium site however, the active site density will be added directly into the model as the loading is not known.

The model was optimised based on the experimental data from the stabilised, non-deactivated catalyst sample. The hope is that by calibrating the kinetic constants for the stabilised data, alterations to the dispersion factor and active site density will be adequate to model the ageing procedure and validate the model even to the deactivated samples. Due to the fact that the deactivation process reduces the active sites but generally does not affect the intrinsic rate constant [13]. However, the values set for the active sites will affect the optimisation process in GT-suite of the kinetic rate constants, so setting the right values of the active site density in the beginning might be of high importance.

The optimisation process will begin by calibration of cerium active site density and the reaction parameters for the reactions that take place on the cerium site, the ”OSC reactions”. Following that will be calibration of PGM dispersion factor and the reaction parameters for the reactions on PGM site using the steady state experiments at constant temperature. Finally will be a validation of the optimised model parameters using the light-off experiments. To limit the scope of the thesis, the validation will focus on the results of the light-off experiments for the lean-phase mixture, mixture #8.

4.2.1 Calibration of Cerium sites

To calibrate the Cerium active site density, earlier work such as Onorati et al. [17] utilised experimental lambda measurements at outlet. However, as there was no lambda sensor added on the SGB as well as no experimental outlet values of O_2, no lambda measurements of the outlet were available. For this reason, the Cerium active site density could not be calibrated and a set value was chosen based and same was used throughout all experiments. For future studies, the oxygen concentration could have been quantified using the oxygen storage experiments, however this action was not performed in this thesis.

The next step was to optimise the reactions on the cerium site (Reactions #10-15 in Table 4.1), which was to be done utilising the OSC experiments. The original optimisation plan aimed at utilising OSC experiment 1 to optimise reaction #12, and OSC experiment 2 to optimise reaction #10 and #13. Due to missing experimental values of oxygen and hydrogen, as well as not performing any OSC test including C_3H_8, reaction #10, #14 and #15 was left with the baseline parameters. However, after finishing the optimisation completely as described in the sections below and performing the validation on the light-off test, it was shown that the final optimised model had not been optimised in a good way. The optimised model also simulated a conversion of 10-15% of the gas species already at low temperatures, which was not in agreement with experimental values. For example on how the simulation behaved, see Figure 4.3.

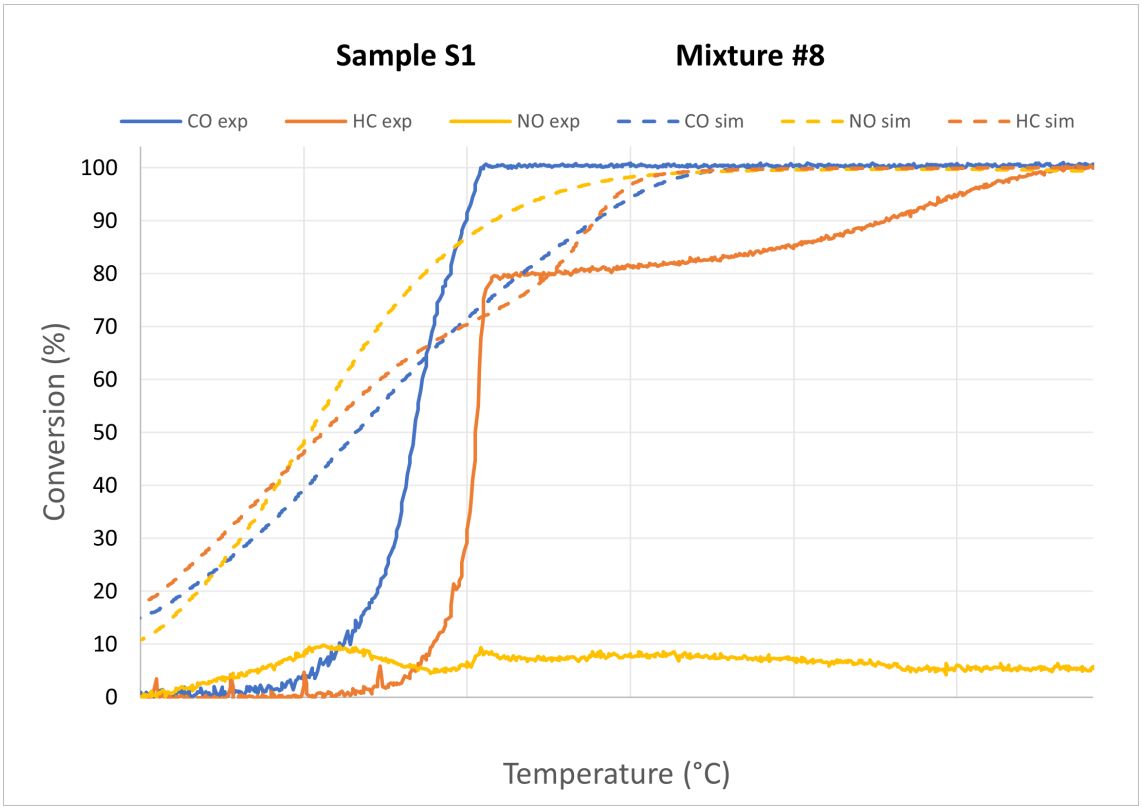

Figure 4.3: The simulated and experimental values after finished optimisation using optimised values for cerium site (and PGM site) reactions. Simulated on the light-off test for mixture #8. ΔT is 60°C.

Due to these results, it was decided to re-run the optimisation process, but keeping the baseline parameters for the reactions on Cerium site. The following sections will explain the optimisation process and results based on baseline parameters for reaction #10 to #15.

4.2.2 Calibration of PGM site

The PGM dispersion factor was calibrated to match 50% conversion for CO [18] using the baseline reaction rate parameters. In Figure 4.4 the simulated value of CO conversion over temperature for different PGM dispersion factors can be seen.

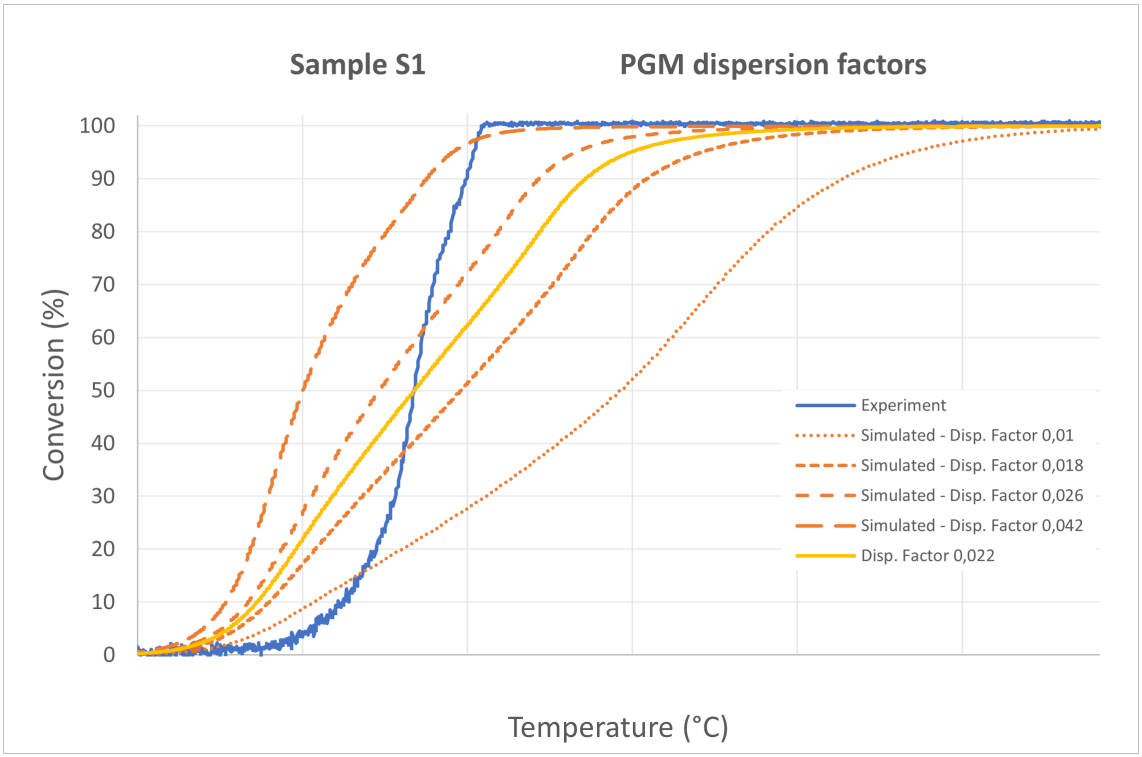

Figure 4.4: Simulated conversion of CO, with baseline parameters, for different values of PGM dispersion factor. ΔT is 60°C.

A value of **0,022** for the PGM dispersion factor of was chosen, a value that seemed low as the ratio of active sites to total sites for the stabilised catalyst sample should be quite high.

The next step was optimisation of the reaction parameters on the PGM sites, reaction #1-#9 in Table 4.1. This was done using the constant temperature steady state experiments. Reaction #4 was never optimised due to the lack of experimental hydrogen values but left with the baseline parameters. Which constant temperature mixtures used to optimise what reactions can be seen in Table 4.4. The order of how the reactions were optimised was decided to minimise the parameters targeted in each optimisation step.

Table 4.4: Table showing which steady state mixtures are targeting which reactions. Highlighted in bold are the mixtures eventually used for optimising the reaction parameters.

Reaction #	Reactants	Products	Mixture for optimisation
1	$CO+0.5O_2$	CO_2	**M2**
2	$C_3H_6+4.5O_2$	$3CO_2+3H_2O$	**M1**, M7
3	$C_3H_8+5O_2$	$3CO_2+4H_2O$	**M1**, M7
4	$H_2+0.5O_2$	H_2O	M2, M7
5	$CO+NO$	$CO_2+0.5N_2$	**M5**
6	C_3H_6+9NO	$3CO_2+3H_2O+4.5N_2$	**M6**
7	H_2+NO	$H_2O+0.5N_2$	**M5**
8	$CO+H_2O$	CO_2+H_2	M2, **M3**, M5
9	$C_3H_6+3H_2O$	$3CO+6H_2$	M1, **M4**, M6, M7

Despite having performed steady state experiments for 5 temperatures, only three of the temperatures were in the end used for optimisation. These being 300°C, 400°C and 500°C. The reason behind this was to save time in the optimisation run, and as the temperature ramp went up to 500°C that was chosen as the maximum temperature.

Below will each of the optimisation steps be describe, which mixture that was used to target what reaction.

Step 1 *Reaction #8:* $CO + H_2O \rightarrow CO_2 + H_2$

The first optimisation step of the kinetic parameters for the PGM site reactions will be explained in more detail. The following optimisation steps followed the same procedure.

As can be seen in Table 4.4, Mixture #3 has only one relevant reaction on the PGM site, this being Reaction #8, and was therefore subject for the first optimisation. The parameters targeted for optimisation was $\mathbf{log([A])}$ and $[\mathbf{E}_A]$. The reason behind using the logarithmic value of the pre-exponential factor [A] was in order to raise the sensitivity of the optimisation process.

CO was included as the only gas specie in the objective function (Eq. 2.12) for this step. The t_{start} in Eq. 2.12 was set for when the experimental outlet values reached steady state. The GA was run first for **15 generations** with a higher range for the parameters. If a convergence was seen in the end of these 15 generations, the optimisation was then re-run with a tighter range for a more accurate response. If there was no convergence after first 15 generations, the optimisation was extended for another 10 generations.

The value of the parameters before and after optimisation are seen in Table 4.5.

Table 4.5: Values of pre-exponential factor and activation energy before and after optimisation run

	Baseline parameters	**After optimisation**
log([A8])	5,255	4,396
[A8]	1,8*10^5	2,492*10^4
[E_A8]	43926.258	39366.836

The result of the simulation versus experiment for the outlet fraction of CO before and after optimising for the different temperatures can be seen in the Figures 4.5 to 4.7. A summary of the conversion at different temperatures using baseline parameters, optimised parameters and the experimental values is seen in Figure 4.8.

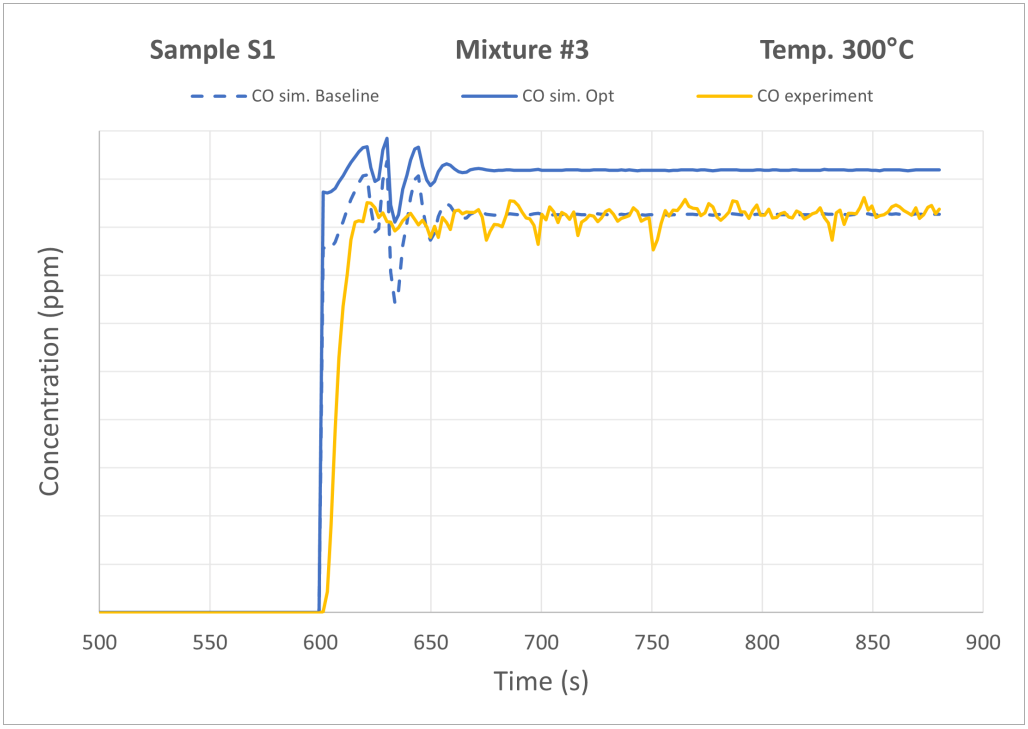

Figure 4.5: Fraction of CO at outlet for 300°C, before optimisation and after optimisation.

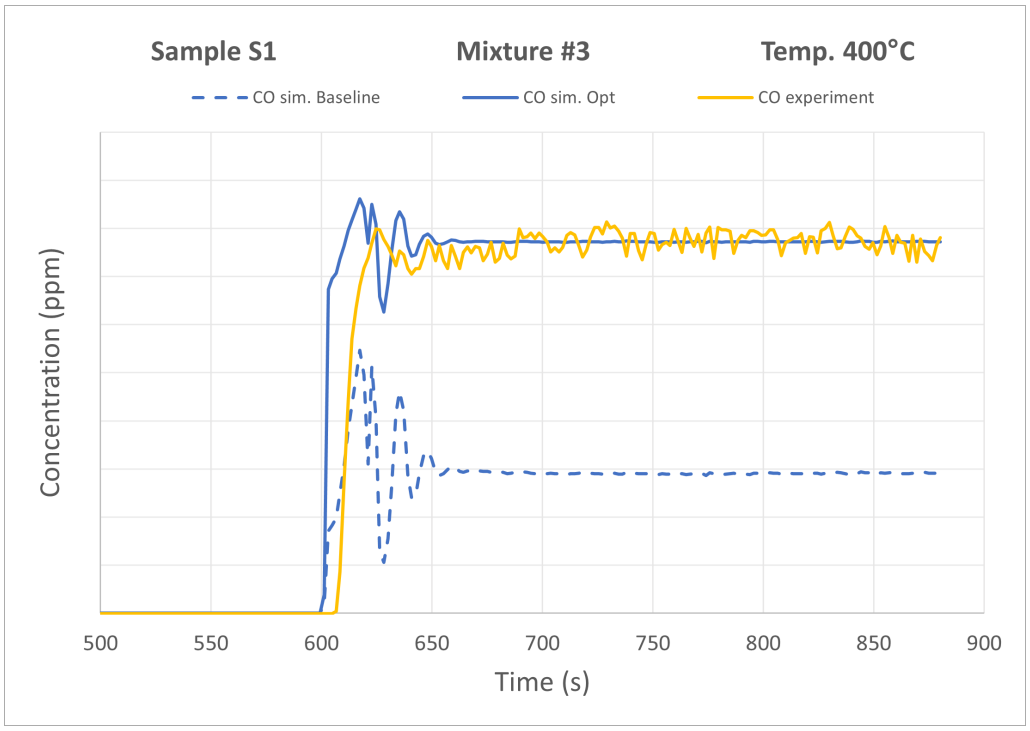

Figure 4.6: Fraction of CO at outlet for 400°C, before optimisation and after optimisation.

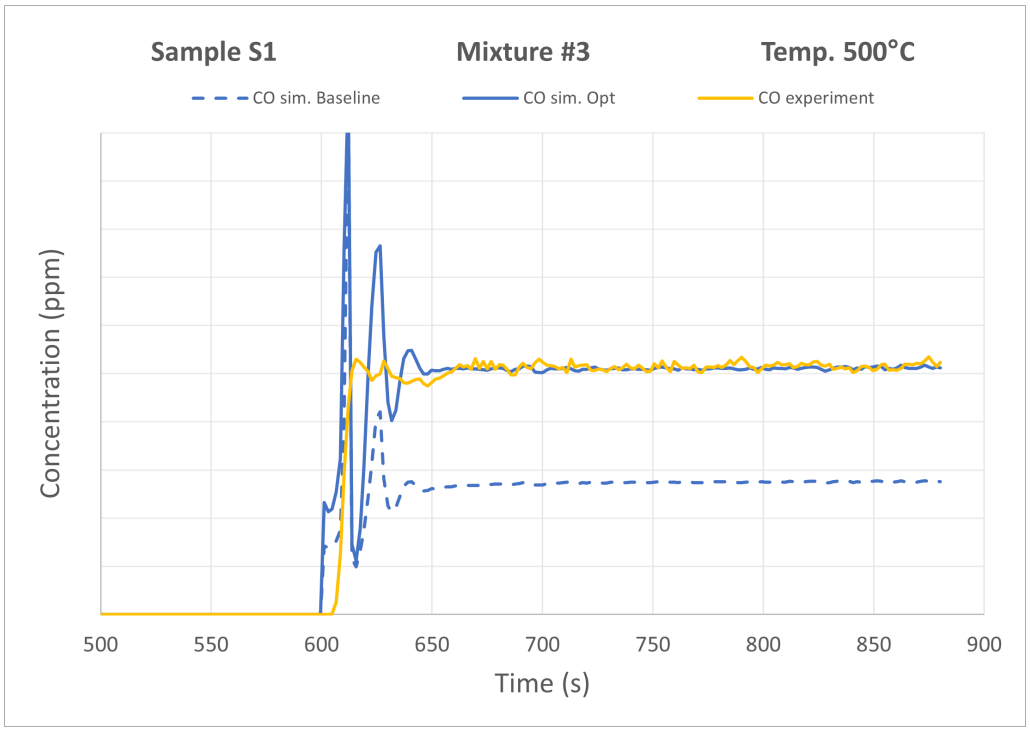

Figure 4.7: Fraction of CO at outlet for 500°C, before and after optimisation.

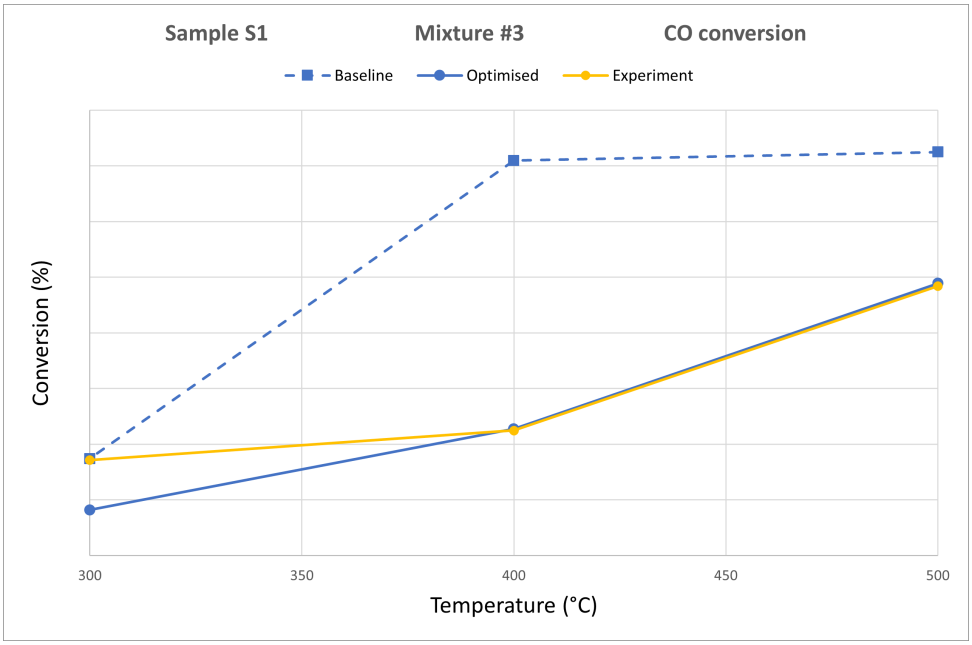

Figure 4.8: Conversion at different temperature, comparing the simulated values using either baseline or optimised parameters, with the experimental result.

As the result show, it was hard to get a good agreement for all three temperatures, and the optimised parameters ended up performing worse at 300°C but better for 400°C and 500°C.

Step 2 *Reaction #9:* $C_3H_6 + 3H_2O \rightarrow 3CO + 6H_2$

Following the same procedure as for Step 1, Mixture #4 was used to optimise the kinetic parameters for reaction 8. For this optimisation both CO and hydrocarbons were included in the objective function.

Step 3 *Reaction #5:* $CO + NO \rightarrow CO_2 + N_2$
Reaction #7: $H_2 + NO \rightarrow H_2O + 0,5N_2$

As reaction #8 had already been optimised based on M3, the reactions left connected with Mixture #5 are reaction #5 and #7. Due to both reaction having a reducing effect of NO, it was decided to optimise both at the same time, leading to 4 parameters for optimisation. The objective function was set to include CO and NO.

Step 4 *Reaction 6:* $C_3H_6 + 9NO \rightarrow 3CO_2 + 3H_2O + 4,5N_2$

Similarly as for mixture #5, for mixture #6 one reaction of influence had already been optimised (Reaction #9), leaving reaction #6 left and therefore subject of optimisation. In this case NO and THC was used as species in the optimisation process.

Step 5 *Reaction #1:* $CO + 0,5O_2 \rightarrow CO_2$

Mixture #2 was used to optimise only reaction #1, as reaction #8 had already been optimised and reaction #4 was left with baseline parameters due to the lack of hydrogen measurements. Reaction #1 was optimised with CO in the objective function. The earlier steps had shown big improvements in the match between experimental and outlet measurements after optimisation, however the results were not as promising for mixture #2.

As can be seen in Figures 4.9, 4.10 and 4.11, the experiment at 500°C did not see any improvement after optimising, while there was a slight improvement for 400°C and a good match for 300°C. Once again it was hard to find parameters that would fit the data at all temperatures. Reaction #8 was believed to possibly have high influence and since it was not optimised for mixture #2, that could be an explanation. However, when letting reaction #8 optimise on mixture #2 instead of mixture #3, no improvement was seen for mixture #2. It can also be seen that the experimental data is showing a delay from when the mixture enter the system at 600 seconds before it was detected at the outlet. This is believed to be because of CO storage on cerium sites (see reaction #12).

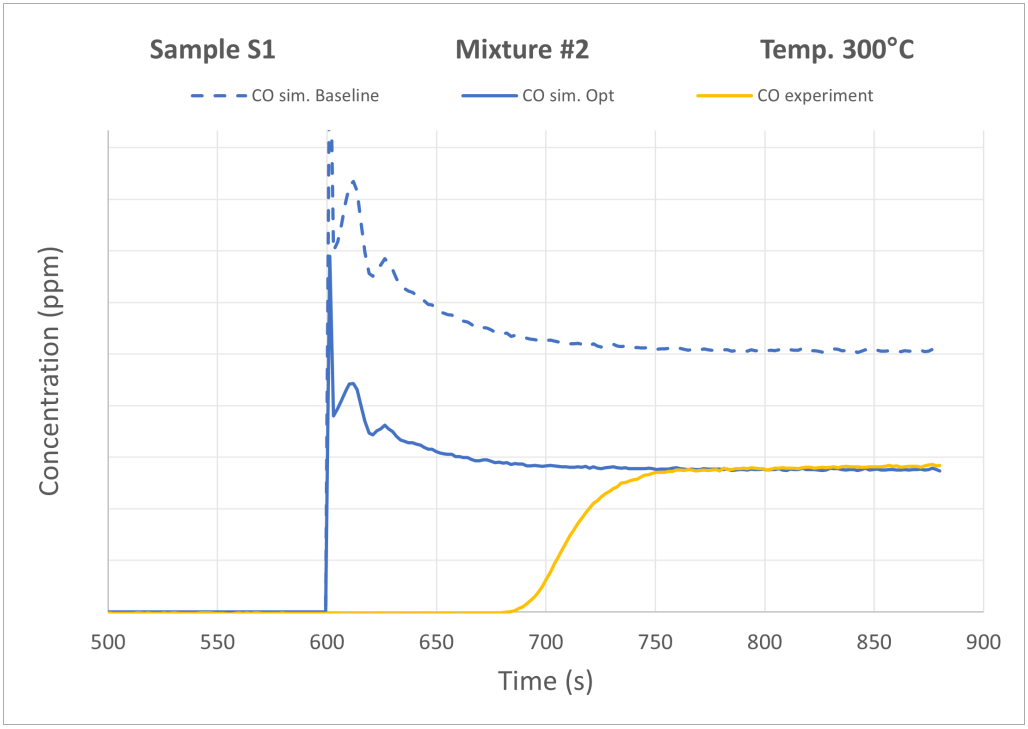

Figure 4.9: Fraction of CO at outlet for mixture #2 at 300°C, before optimisation and after optimisation.

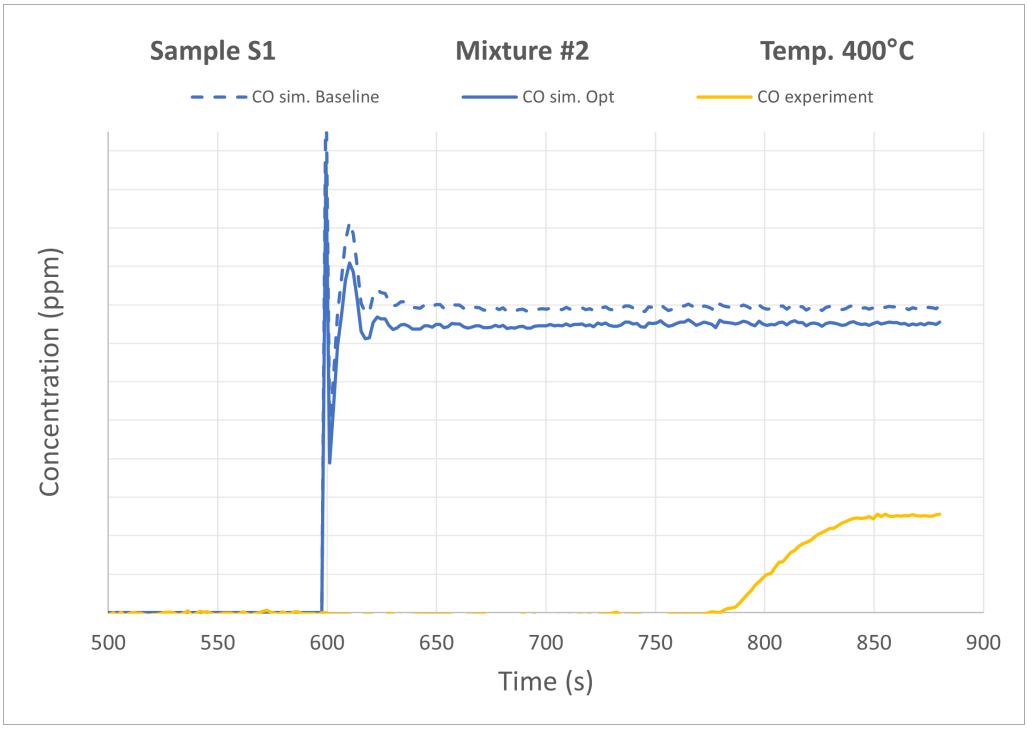

Figure 4.10: Fraction of CO at outlet for mixture #2 at 400°C, before optimisation and after optimisation.

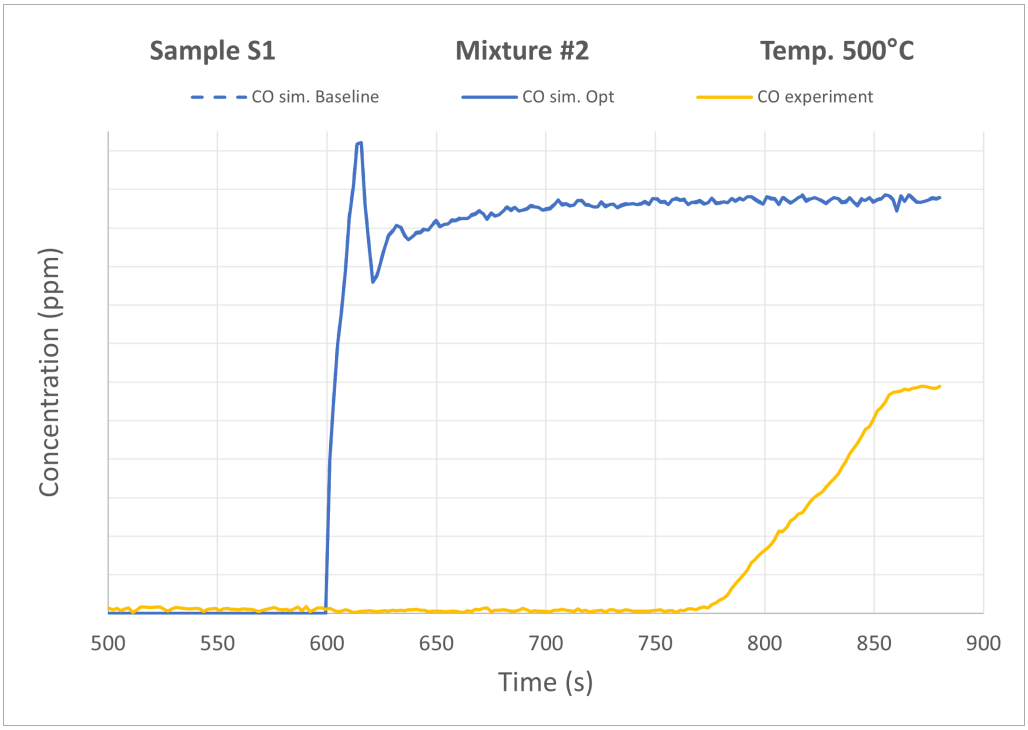

Figure 4.11: Fraction of CO at outlet for mixture #2 at 500°C, before and after optimisation

Step 6 *Reaction #2:* $C_3H_6 + 4,5O_2 \rightarrow 3CO_2 + 3H_2O$
Reaction #3: $C_3H_8 + 5O_2 \rightarrow 3CO_2 + 4H_2O$

As can be seen in Table 4.4, both mixture #1 and mixture #7 could be used for the optimisation process of reaction #2 and #3. Two separate optimisation runs where therefore proceeded, one where the reactions were optimised on the basis of mixture #1, and one for mixture #7. When validating against the temperature ramp test the parameters optimised on mixture #1 showed the best result and was therefore favoured.

4.3 Validation of Parameters

When the optimisation of the kinetic model parameters were finished, the new model were to be validated against the temperature ramp test. The results from before and after the optimisation can be seen in the coming figures. The validation will be focused on using the result from the lean phase light-off (Mixture #8).

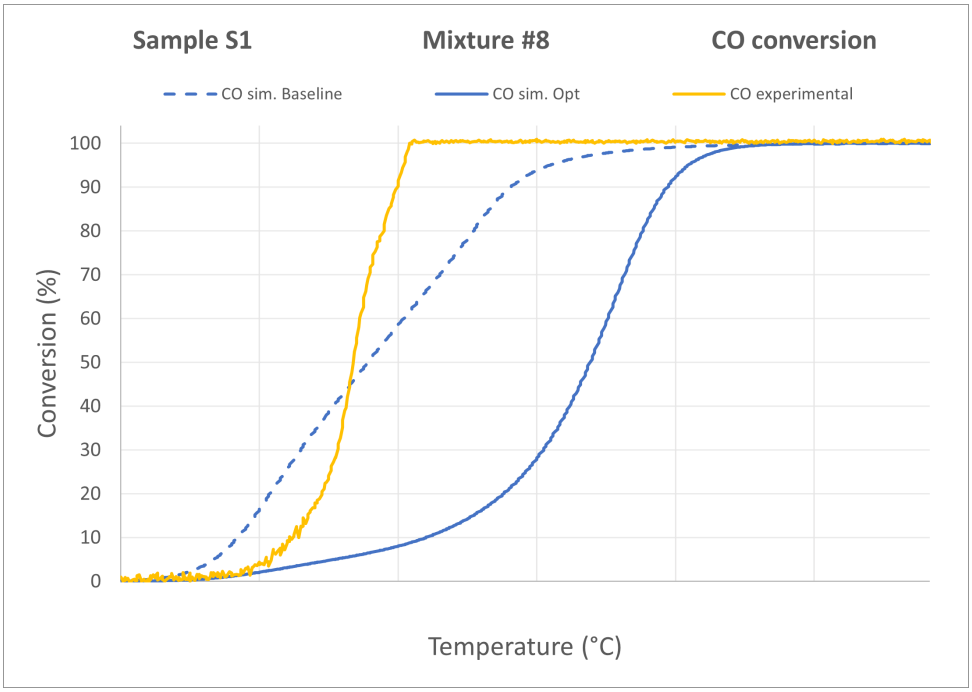

Figure 4.12: Experimental and simulated conversion of CO versus temperature, before and after the optimisation of the kinetic parameters, with a PGM dispersion factor of 0,022. ΔT is 60°C.

In general the optimised parameters performed worse than the baseline parameters, simulating higher light-off temperatures. For the oxidation of CO (see Figure 4.12, the optimised parameters provides a conversion curve more similar to the experimental values than the baseline parameters, however simulates an almost 120°C higher light-off temperature. For the oxidation of the hydrocarbons the shape and predicted light-off temperature match better with baseline parameters, while for the reduction of NO the prediction is better with the optimised parameters.

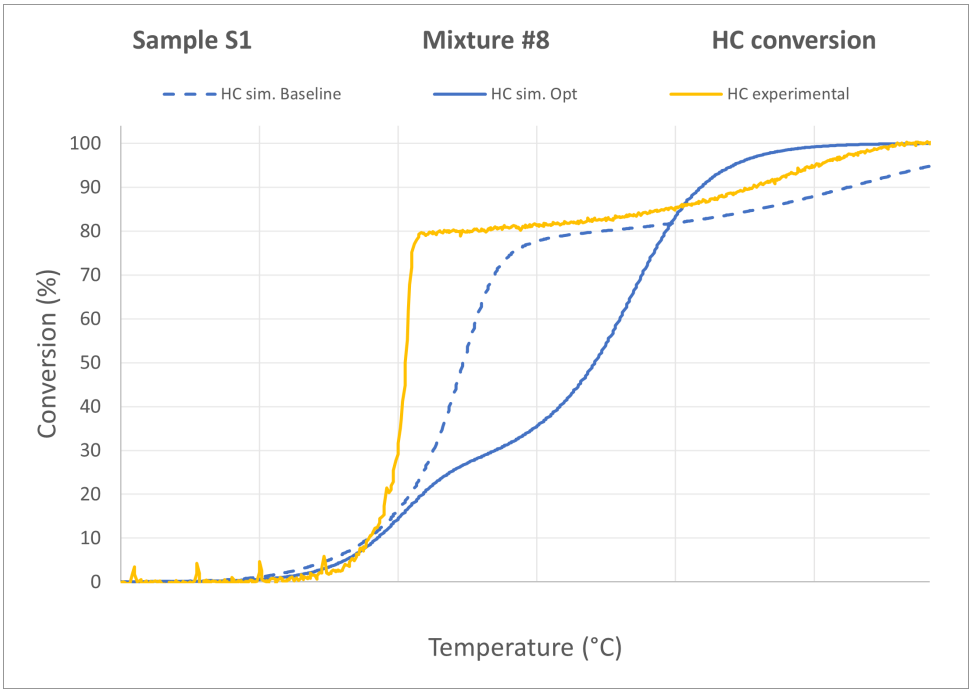

Figure 4.13: Experimental and simulated conversion of HC versus temperature, before and after the optimisation of the kinetic parameters, with a PGM dispersion factor of 0,022. ΔT is 60°C.

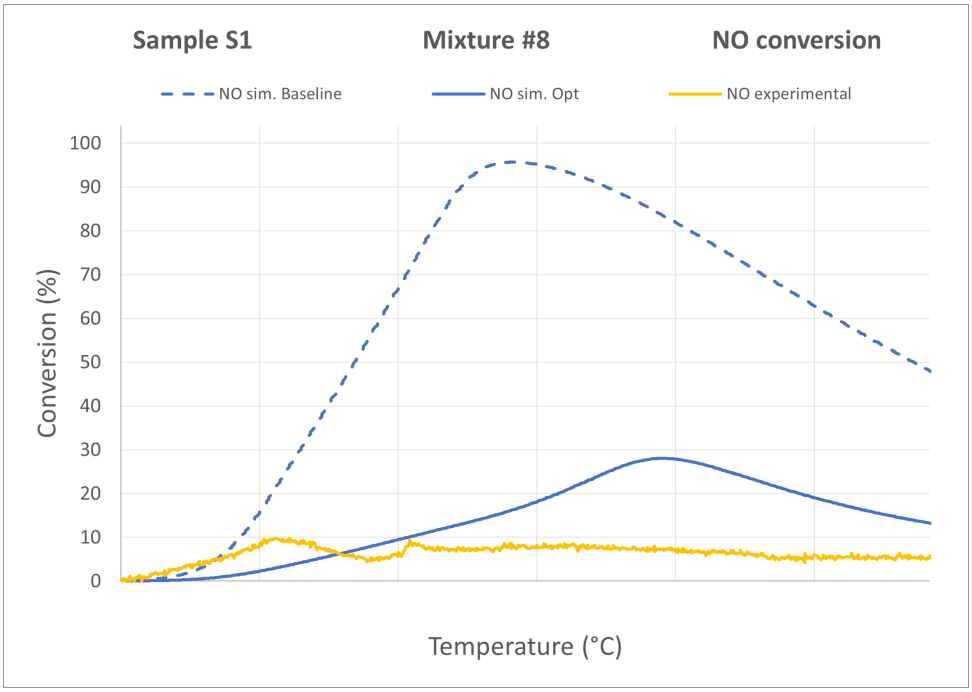

Figure 4.14: Experimental and simulated conversion of NO versus temperature, before and after the optimisation of the kinetic parameters, with a PGM dispersion factor of 0,022. ΔT is 60°C.

4.3.1 Optimisation with Higher PGM Dispersion Factor

A second optimisation run was performed with a PGM dispersion factor of 0.1, to investigate any improvements by use of a higher factor. Using this dispersion factor did mean that the 50% conversion rate of CO did not match up before the optimisation process.

These results showed slight improvement for the predicted light-off temperature for CO and HC-conversion, but showed the same trend as the previous results of the simulation predicting a higher light-off temperature. However assuming a higher light-off temperature is better than simulating a lower, since it will not lead to an overestimation of the catalyst performance.

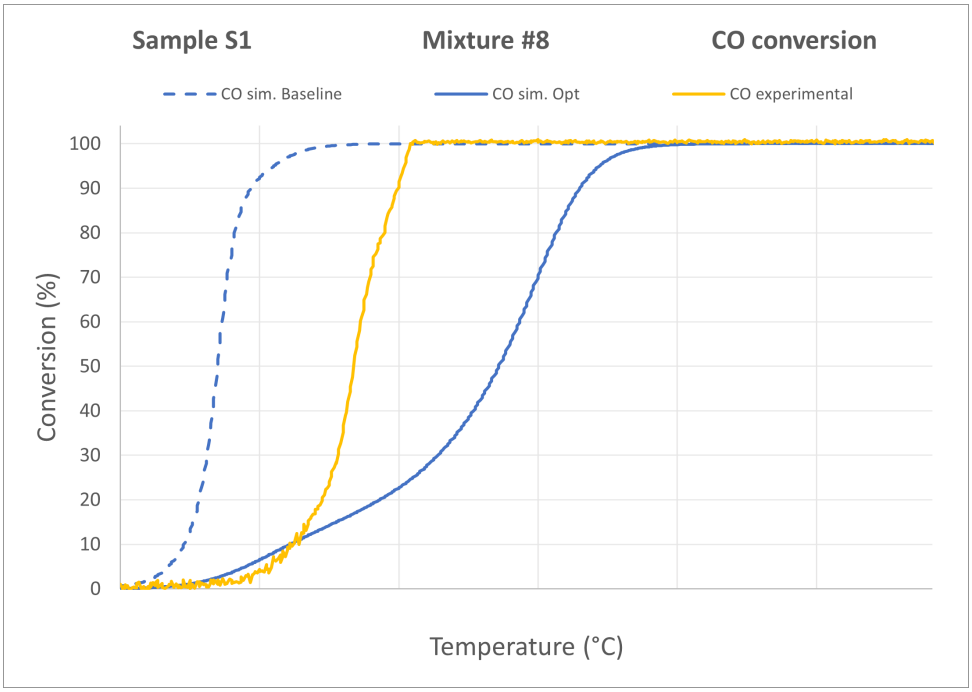

Figure 4.15: Experimental and simulated conversion of CO versus temperature, before and after the optimisation of the kinetic parameters, with a PGM dispersion factor of 0,1. ΔT is 60°C.

Despite not reaching a satisfactory simulation model for the stabilised catalyst sample, it was decided to still investigate how the model worked on the deactivated catalyst samples as well as the engine bench test results. As optimisation process of using a PGM of 0,1 showed slight improvement from the earlier optimisation with 0,022, the model parameters from this is decided to be kept and used for the further simulation.

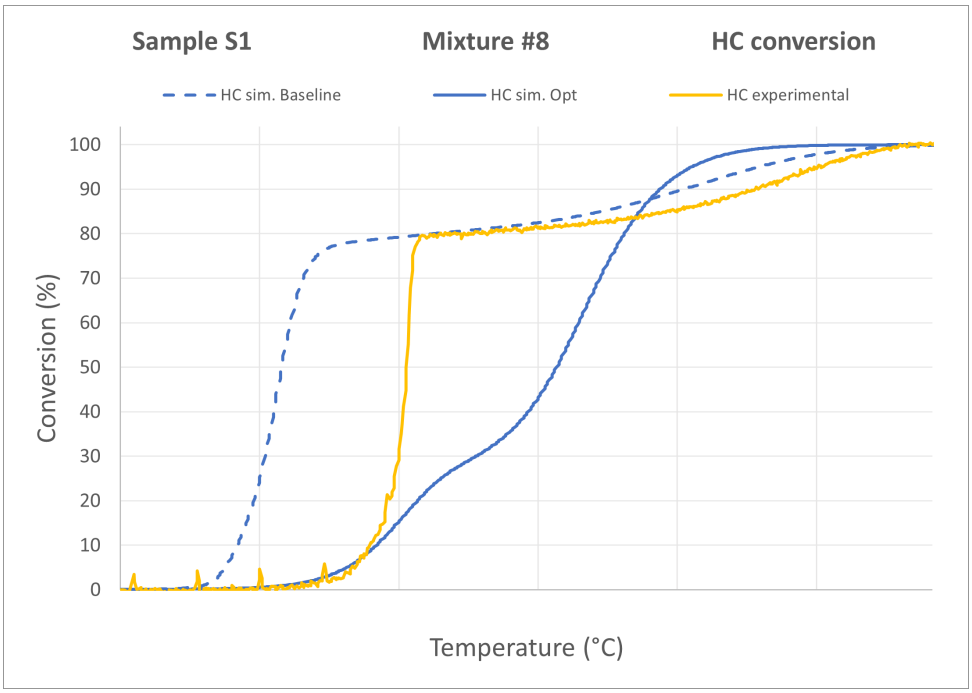

Figure 4.16: Experimental and simulated conversion of HC versus temperature, before and after the optimisation of the kinetic parameters, with a PGM dispersion factor of 0,1. ΔT is 60°C.

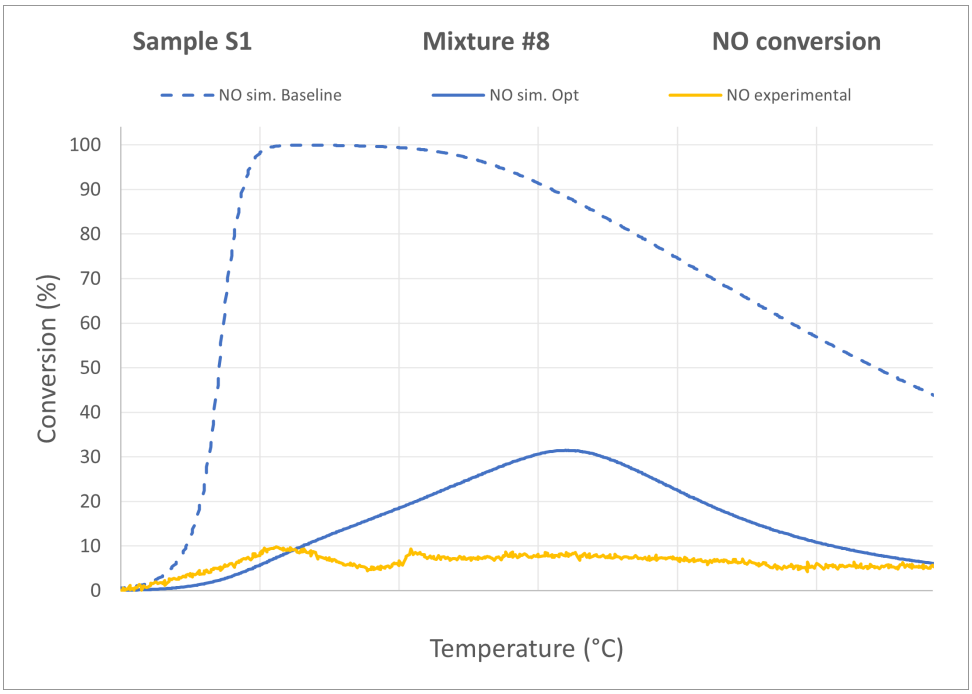

Figure 4.17: Experimental and simulated conversion of NO versus temperature, before and after the optimisation of the kinetic parameters, with a PGM dispersion factor of 0,1. ΔT is 60°C.

4.3.2 Simulation Model with Deactivated Catalyst Samples

Next step was to investigate whether kinetic parameters optimised on a stabilised catalyst can be directly used to model a deactivated sample of same type of catalyst. The simulation will be compared to the results from the front side of the catalyst, Cf1.

As discussed earlier it is assumed that some alterations would have to be done to the PGM dispersion factor as well as Cerium active site density. However when seeing the results, the optimised parameters fit the data without changing the PGM dispersion factor, especially for the oxidation of CO. This gives an indication that perhaps the settings of the deactivation parameters were more tuned to fit an aged catalyst compared to a stabilised one.

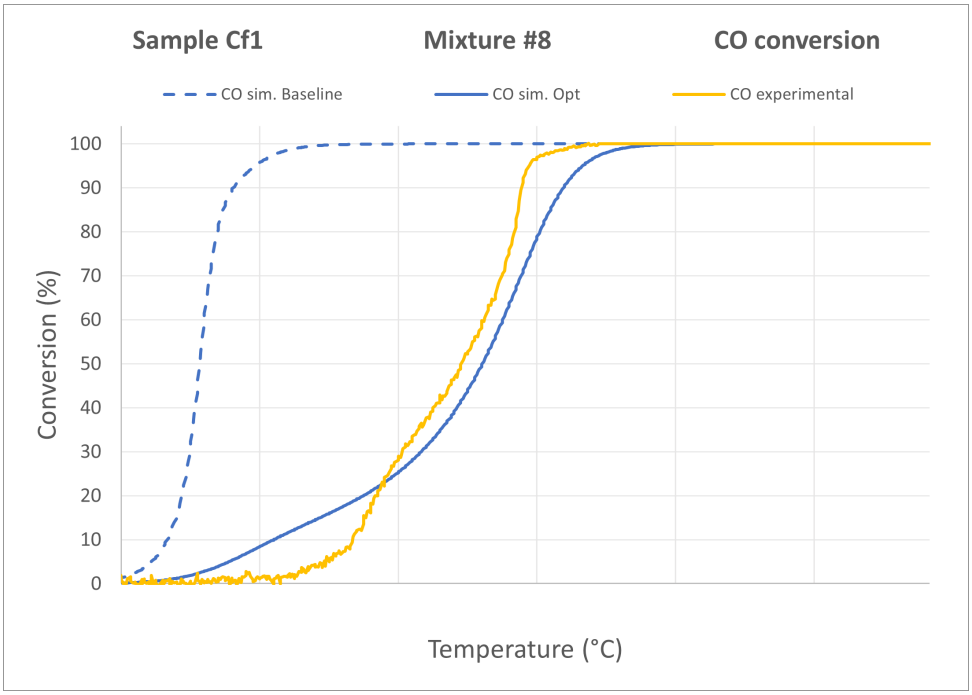

Figure 4.18: Experimental and simulated conversion of CO versus temperature for Cf1 catalyst sample, before and after the optimisation of the kinetic parameters, with a PGM dispersion factor of 0,1. ΔT is 60°C.

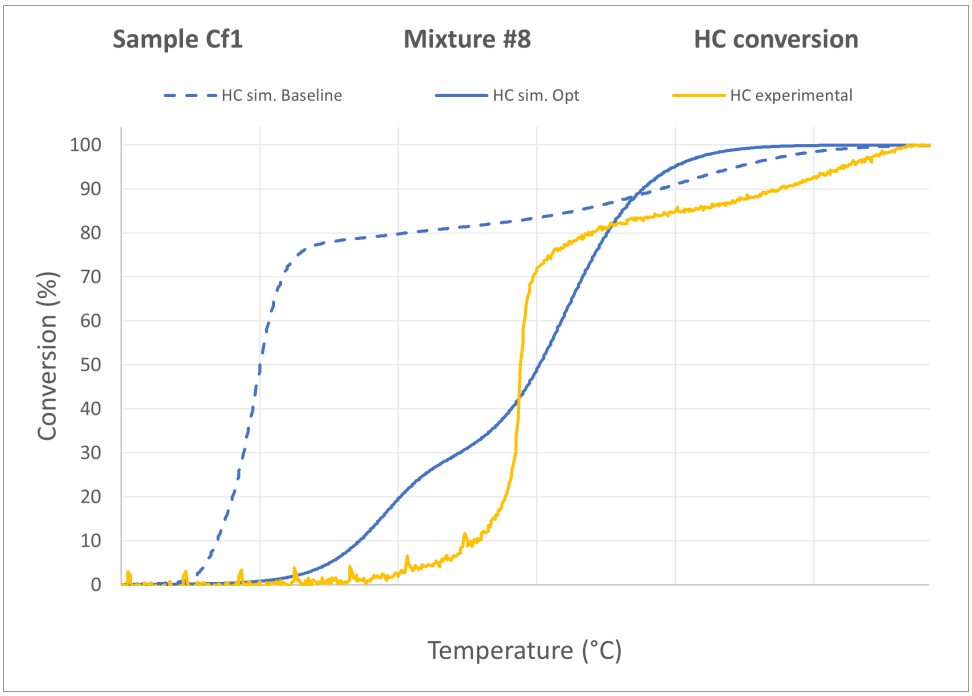

Figure 4.19: Experimental and simulated conversion of HC versus temperature for Cf1 catalyst sample, before and after the optimisation of the kinetic parameters, with a PGM dispersion factor of 0,1. ΔT is 60°C.

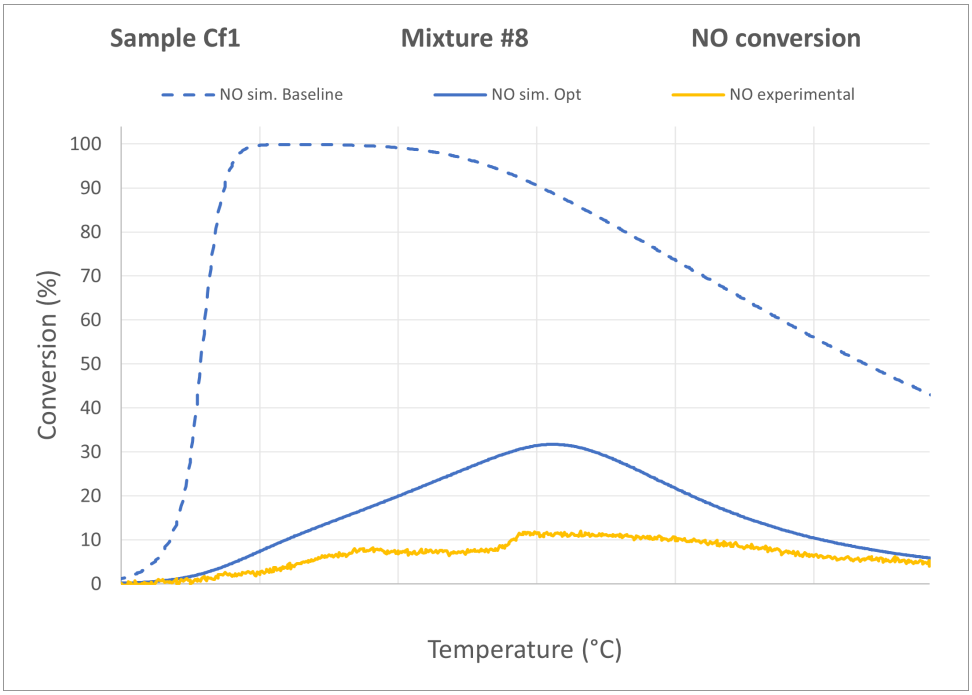

Figure 4.20: Experimental and simulated conversion of NO versus temperature for Cf1 catalyst sample, before and after the optimisation of the kinetic parameters, with a PGM dispersion factor of 0,1. ΔT is 60°C.

4.3.3 Simulation Model based on Motor Bench Experiment

The final model parameter test was done on the values from the engine bench test explained in Section 3.1, in order to see how well a model based on SGB experiment could work simulating engine bench tests.

Looking at the figures below, the optimised parameters shows some show improvement, especially for the shape of the conversion curves even though it is not predicting the light-off temperatures correctly. Worth to mention here is that no change has been done to the deactivation parameters.

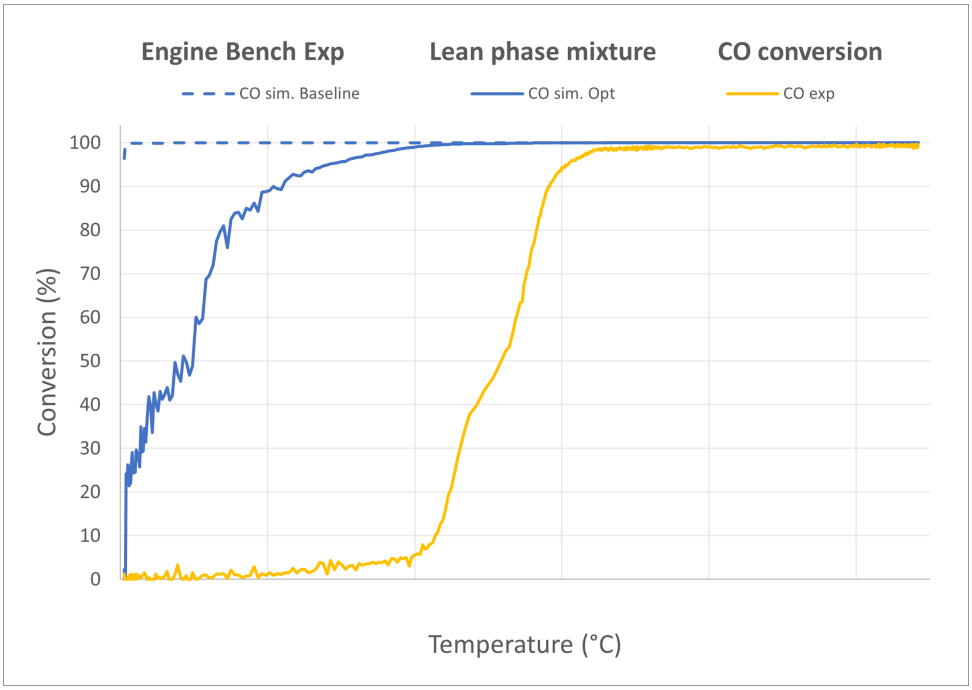

Figure 4.21: Experimental and simulated conversion of CO versus temperature for motor bench test, before and after the optimisation of the kinetic parameters, with a PGM dispersion factor of 0,1. ΔT is 60°C.

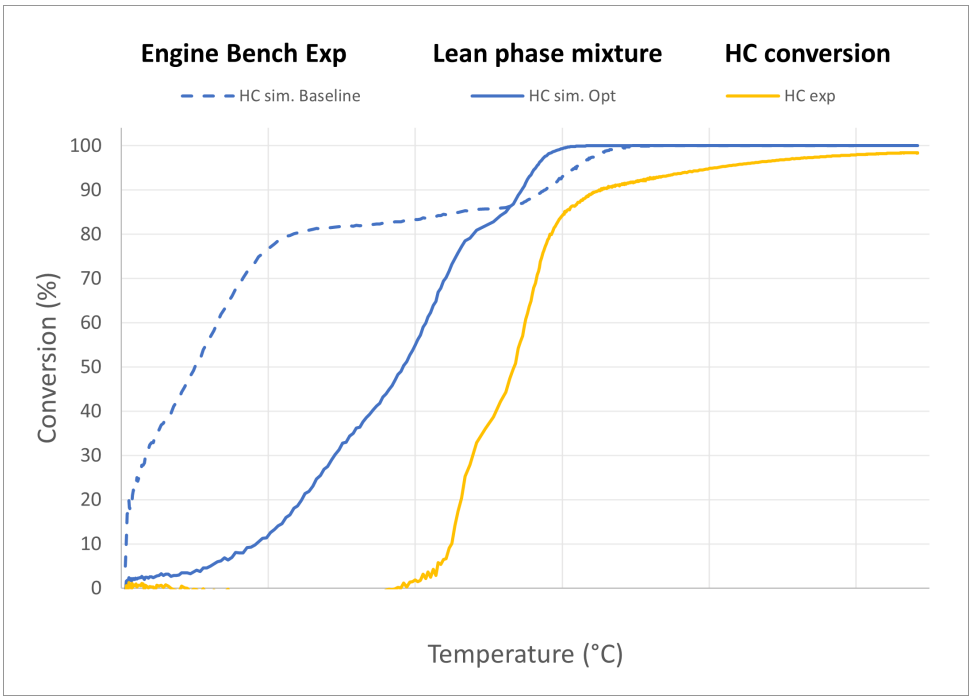

Figure 4.22: Experimental and simulated conversion of HC versus temperature for motor bench test, before and after the optimisation of the kinetic parameters, with a PGM dispersion factor of 0,1. ΔT is 60°C.

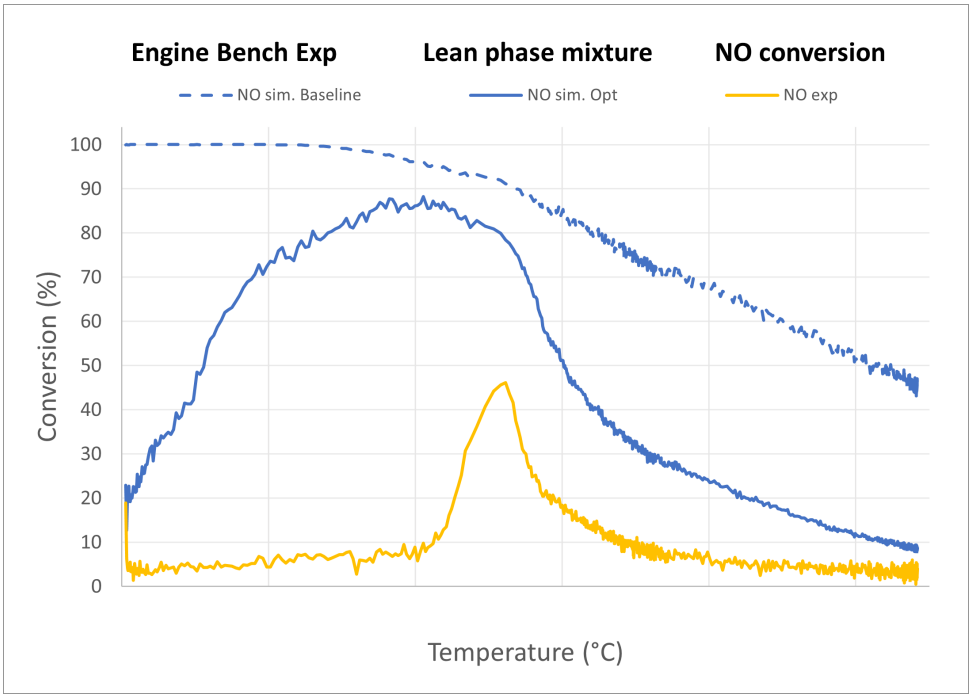

Figure 4.23: Experimental and simulated conversion of NO versus temperature for motor bench test, before and after the optimisation of the kinetic parameters, with a PGM dispersion factor of 0,1. ΔT is 60°C.

4.3.4 Effect of PGM Dispersion Factor

To further study the effect of the PGM dispersion factor, the deactivated front sample was modelled with the optimised parameters found in the first optimisation, where a PGM dispersion factor of 0,022 was used. The PGM dispersion factor was then changed until the simulated conversion rate fit the experimental data, and the result can be seen in Figure 4.24.

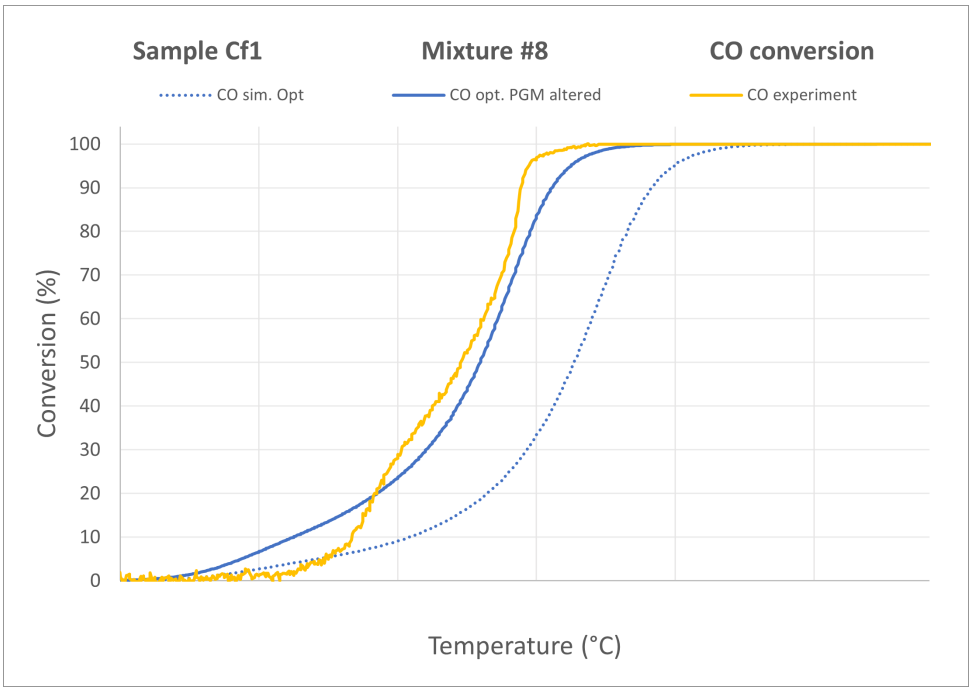

Figure 4.24: Experimental and simulated conversion of CO, where the PGM dispersion factor has been altered to fit the experimental value. ΔT is 60°C.

With this method a PGM dispersion factor of 0,05 was found that gave as good as result as can be seen in Figure 4.18 which used the model parameters optimised for a PGM factor of 0.1. Despite two different PGM factors and slightly different values for the model parameters, both simulations showed the same result.

5

Conclusion

In this master thesis a stabilised and a deactivated catalyst has been investigated by performing SGB experiments. This with the aim to gather experience of calibration the simulation tool build in to the GT suite package. The results of the SGB experiments provided experience in the (expected) axial difference in characteristic of an aged catalyst. An engine bench aged catalyst in the here investigated case is exposed for more poison in the front and more thermal exposure in the rear part. Also in vehicle ageing a axial ageing profile will occur. Usage of the simulation tool needs to consider this insight and for a future case, bench ageing method development can potentially be supported from simulation tool characterisation.

It is expected to have to alter the PGM dispersion factor depending on the deactivation of the catalyst, however the value of the PGM dispersion factor that will fit the data depends on what factor it was optimised on first, see Section 4.3.4. As seen in Section 4.2.2, when optimising based on constant temperature experiments, it was hard to get an agreement for all the temperature. It could be that using temperature ramp test instead would increase the performance of the model, as it would cover a wider temperature range.

The evaluation of the model parameters for light off simulation was limited to the lean case (lambda=1,02). When the dispersion factor was tuned in a second step, with a PGM dispersion factor of 0,1, the optimised parameter case had slightly better accordance in the experimental results than the base case parameters. However it was under predicting a little bit. With the aged case the accordance with the developed parameters were much better accordance in the experimental results than with the base case (here the base case parameters over predicted in an unacceptable way.). In general however the baseline parameters are showing a good accordance with the experimental values, showing that perhaps a full optimisation of all the model parameters are not necessary. It might be that focusing on altering other parameters, such as the inhibition functions that were not covered in this report, will be adequate enough to acquire a good simulation model.

Although this report did not find an optimised model based on the experimental results, it still had the opportunity to investigate factors needed for a good simulation model. It showed that the baseline parameters provided a good simulation without the need of optimisation, especially for the oxidation of hydrocarbons. It

can therefore be concluded that further investigations is desired to quantify how crucial the need of unique experimental parameter setting actually is.

5.1 Future studies

To further improve the simulation, there are multiple factors that would be of interest to investigate. In an earlier thesis by Castellano G. [19], five more reactions were added in the model on the cerium site. It is possible that adding and calibrating these would give a more correct simulation and should be investigated. Another improvement could be including temperature ramp test for the separate mixtures instead of constant temperature test. It is also possible that a more manual calibration exploiting the linear regression of Arrhenius equation would provide a better optimisation. However that would only applied if using constant temperature test and not temperature ramps.

In the optimisation process, it was decided to optimise based on the total values of hydrocarbons and not propane and propylene separately. For a more exact calibration it would probably be beneficial to look into optimising them separately instead, especially when individual experimental values are available. Same can be discussed for the precious metal sites, as the Palladium and Rhodium metals are affected differently in the deactivation process. In this project they were calibrated together with one active site density, so a future improvement could be to instead simulate them to separately.

Seeing as the front and rear side of the catalyst showed different levels of deactivation, it would be of interest to investigate simulating slices of the catalyst brick instead of the whole brick. This could potentially give a more correct simulation for a deactivated catalyst, but also give insight in how to plan the rapid ageing method for future studies. However, it is important that the final model has a good agreement before studying the potential usage of planning deactivation methods.

Bibliography

[1] Rutger A. Van Santen. *Modern Heterogeneous Catalysis: An Introduction*, chapter 2, pages 167–200. wiley, 1 2017. ISBN 9783527694501. doi: 10.1002/9783527810253.

[2] UMICORE Automotive Catalysts. Three-way catalyst. URL `https://ac.umicore.com/en/technologies/three-way-catalyst/`. accessed 2022-06-01.

[3] Karthik Ramanathan and Chander Shekhar Sharma. Kinetic parameters estimation for three way catalyst modeling. *Industrial and Engineering Chemistry Research*, 50:9960–9979, 9 2011. ISSN 08885885. doi: 10.1021/ie200726j.

[4] Ronald M. Heck and Robert J. Farrauto. Automobile exhaust catalysts. *Applied Catalysis A: General*, 221:443–457, 11 2001. ISSN 0926-860X. doi: 10.1016/S0926-860X(01)00818-3.

[5] Jihui Wang, Hong Chen, Zhicheng Hu, Mingfa Yao, and Yongdan Li. A review on the pd-based three-way catalyst. *Catalysis Review*, 57(1):79–144, 2014. doi: 10.1080/01614940.2014.977059.

[6] Shawn Rood, Salvador Eslava, Alexis Manigrasso, and Chris Bannister. Recent advances in gasoline three-way catalyst formulation: A review. *SAGE Journal*, 234(4):936–949, June 2019. ISSN 09544070. doi: 10.1177/0954407019859822.

[7] Sheng Su, Yitu Lai, Chunxiao Hao, Pan Hou, Tao Lv, and Yunshan Ge. Review of rapid ageing testing methods of three-way catalyst for gasoline engine. *International Journal of Vehicle Performance*, 6:277–293, 2020. ISSN 17453208. doi: 10.1504/IJVP.2020.109179. URL `https://www.researchgate.net/publication/344089167_Review_of_rapid_ageing_testing_methods_of_three-way_catalyst_for_gasoline_engine`.

[8] Martyn V. Twigg. Catalytic control of emissions from cars. *Catalysis Today*, 163:33–41, 4 2011. ISSN 0920-5861. doi: 10.1016/J.CATTOD.2010.12.044.

[9] Raffael Hedinger, Philipp Elbert, and Christopher Onder. Optimal cold-start control of a gasoline engine. *Energies 2017, Vol. 10, Page 1548*, 10:1548, 10 2017. ISSN 19961073. doi: 10.3390/EN10101548. URL `https://www.mdpi.com/1996-1073/10/10/1548/htmhttps://www.mdpi.com/1996-1073/10/10/1548`.

[10] Jonathan Lock, Kristoffer Clasén, Jonas Sjöblom, and Tomas McKelvey. Cold-start modeling and on-line optimal control of the three-way catalyst. *Emission Control Science and Technology*, 7:321–347, 4 2021. ISSN 21993637. doi: 10.1007/s40825-021-00199-x. URL https://arxiv.org/abs/2104.12390v1.

[11] Liam Mc Grane, Roy Douglas, Kurtis Irwin, Jonathan Stewart, Andrew Woods, and Fabian Muehlstaedt. A study of the effect of light-off temperatures and light-off curve shape on the cumulative emissions performance of 3-way catalytic converters. SAE International, 4 2021. doi: 10.4271/2021-01-0594.

[12] Theophil S. Auckenthaler. Modelling and control of three-way catalytic converters. 2005. doi: 10.3929/ethz-a-005011053. URL https://doi.org/10.3929/ethz-a-005011053.

[13] J. A. Moulijn, A. E. Van Diepen, and F. Kapteijn. Catalyst deactivation: is it predictable?: What to do? *Applied Catalysis A: General*, 212:3–16, 4 2001. ISSN 0926-860X. doi: 10.1016/S0926-860X(00)00842-5.

[14] Saeed Abdolmaleki, Omid Abianeh, and Javad Roudaki. A review of the automotive three-way catalyst ageing technology. 10 2009.

[15] S.N. Sivanandam and S.N. Deepa. *Genetic Algorithms*, pages 15–37. Springer Berlin Heidelberg, Berlin, Heidelberg, 2008. ISBN 978-3-540-73190-0. doi: 10.1007/978-3-540-73190-0_2. URL https://doi.org/10.1007/978-3-540-73190-0_2.

[16] Jian Gong, Di Wang, Junhui Li, Krishna Kamasamudram, Neal Currier, and Aleksey Yezerets. An experimental and kinetic modeling study of aging impact on surface and subsurface oxygen storage in three-way catalysts. *Catalysis Today*, 320:51–60, 2019. ISSN 0920-5861. doi: https://doi.org/10.1016/j.cattod.2017.11.038. URL https://www.sciencedirect.com/science/article/pii/S0920586117308179. SI:Vehicle Emissions Catalys.

[17] Angelo Onorati, Augusto Della Torre, Gianluca Montenegro, Stefano Paltrinieri, Federico Rulli, and Vincenzo Rossi. Calibration of the oxygen storage reactions for the modeling of an automotive three-way catalyst. *Industrial and Engineering Chemistry Research*, 60:6653–6661, 5 2021. ISSN 15205045. doi: 10.1021/ACS.IECR.0C05744/. URL https://pubs.acs.org/doi/full/10.1021/acs.iecr.0c05744.

[18] Gamma Technologies. *Exhaust Aftertreatment Application Manual*. 2021.

[19] Giuseppe Castellano. Calibration of an automotive three-way catalyst model based on synthetic gas bench experiments, 10 2021.

DEPARTMENT OF SOME SUBJECT OR TECHNOLOGY
CHALMERS UNIVERSITY OF TECHNOLOGY
Gothenburg, Sweden
www.chalmers.se

CHALMERS
UNIVERSITY OF TECHNOLOGY